April 1986 LIDS-R-1549

MASSACHUSSETTS INSTITUTE OF TECHNOLOGY

LABORATORY FOR INFORMATION AND DECISION SYSTEMS

REPORT ON

ACOUSTIC TELEMETRY NETWORKING

for the period July 1, 1984 to August 31, 1985

by

Prof R.G. Gallager
Prof P.A. Humblet
Whay Lee
Wen K. Han

This research was supported in its entirety by the Charles Stark Draper Laboratory

1) INTRODUCTION

This report studies some networking problems that are relevant to a communication system for use by a small fleet of submarines involved in detection and tracking operations. The fleet may consist of between 3 and 5 platforms separated by about 15 km and moving in formation at about 5 km/h. Communication between the submarines takes place on a sonar channel at a yet to be specified frequency between 1000 and 40000 Hz. The requirements for the data rate are between 10 and 100 bps. Low probability of intercept is a key requirement and spread spectrum modulation will be used. The determination of many operational parameters will depend on an ongoing study of wave propagation performed at CSDL and MIT's Department of Ocean Engineering.

Aspects of the study

We have focused our attention on three aspects of the system:
-channel sharing methods
-data routing patterns
-combination of coding and automatic repeat request (ARQ) for low probability of intercept (LPI) operations.

Details about these three aspects are developed below. Before giving more details we will recall some physical parameters that determine many characteristics of the system.

Physical characteristics

Wavelenth: The speed of sound in water is about 1500 m/s, depending on depth, temperature, salinity etc... The wavelength corresponding to a frequency of 1000 Hz is about 1.5 m, while the wavelenght corresponding to 20 khz is 7.5 cm. Especially at the higher frequency, the wavelength is reminiscent of those associated with microwave operation in the air or in space and high antenna gains can be achieved with moderately sized antennas.

Propagation delay: It takes about 10 s for a soundwave to propagate in water between platforms separated by 15 km. This is an unusually large delay for communication systems. However this represents only 1000 "bit times" if transmission takes place at 100 bps.

Attenuation: Waves attenuate as a function of distance. The dependence of the field strength with distance r is of the form $1/r^2 \exp(-a\, r)$. The constant a, which represents attenuation due to absorbtion, varies with frequency. It is about equal to 10^{-3} db/km at 100 Hz, 10^{-1} at 1000 Hz, 1 db at 10 khz and 3.5 dB at 20 khz; these numbers are approximate as they depend on temperature, depth, salinity etc...

Multipath propagation: The velocity gradient of the ocean causes the sound beam to be refracted, causing multipath propagation and fading. Geometric propagation models based on the thermal gradient predict that in ocean deeper than 1 km many propagation paths caused only by refraction will have propagation times within 350 ms of the fastest ray. In addition to those, other paths undergo bottom or surface bounces; their extra delays are much higher, the precise values depend on the depth of operation and on the depth of the ocean.

As if this was not enough, closely spaced multipath distortion (time smear) also occurs because of forward scattering in the medium. This scattering is the result of the thermal microstructure of the water. The signal is also subject to random fluctuating Doppler shifts and spread because of surface and internal wave motion.

Effects due to the movement of the platforms: No significant doppler shift is expected from the movement of the patforms, as they will move in formation. If their speed is 5 km/h (about 1.38 m/s) , this would correspond to about 1 wavelength per second at 1000 hz, and 20 wavelength per second at 20 khz. As fading characteristics change drastically with distance in about half a wavelength, the coherence time of the channel will range from 500 to 25 ms (this assumes that there are scatterers nearby the receiver and may not be very accurate).

2) CHANNEL ACCESS METHOD

This section deals with the way the communication channel should be organized. We immediately distinguish between two main modes of operation:

-) point-to-point, where directional antennas are used to establish point-to-point communication lines between the submarines. If there is little interference between different beams, there is no need to have different transmitters use different frequency bands (FDMA), time slots (TDMA), or different spread spectrum patterns (CDMA).

-) broadcast mode, where omnidirectional antennas are used that allow all the submarines to hear each other. That mode of operation may be advantageous if the same data must be used by many different submarines.
However the broadcast nature of the channel necessitates some precautions in the channel access method to avoid interference.

Among those interference avoiding techniques are FDMA and TDMA. They are not very efficient from a channel use point of view if the data is bursty. There is also the possibility to use contention methods where different transmitters may transmit simultaneously, and collisions are resolved by a protocol. These techniques can be very efficient in situations where it can be quickly determined if a channel is idle, and (ideally) if a collision is occuring, like in ETHERNET.

Initially we were planning to spend a fair amount of time determining the best access method and possibly developing multiaccess protocols. However we quickly realized that point to point communication was preferable. Here are the reasons:

The long propagation times make the efficient determination of channel idleness impossible, except if very long blocks of data are being exchanged. Also the determination of collisions occuring would be a difficult task due to the fading nature of the channel and to the spread spectrum modulation. Thus very efficient contention access did not seem possible. This leaves open the possibility of standard ALOHA, or some type of FDMA, TDMA, or CDMA.

However, the operation in broadcast mode appears undesirable for a number of reasons.
-It may not be required from a data processing point of view.
-Even if it were, reliable communication would be difficult to achieve as the different receivers would see different fading patterns, so that ARQ schemes would be complicated and less efficient than on point to point channels.
- From an LPI viewpoint the operation in broadcast mode is very undesirable as power is transmitted in all directions, giving a big advantage to the interceptor; this can be justified in more details by a method as that in section 3.

The previous remark implies that directional antennas should be used. At the higher frequencies they will have enough directionality so that simultaneous transmissions and receptions can take place at a given platform.

This need not be true at the lower frequencies (with reasonable array size) where the field of view of an antenna may include many transmitters. However in typical situations the transmitters will be at different distances and the section on routing below will explain that information should only be received from the closest transmitter. Interference can still be produced by the farther transmitters. It will be considerably attenuated due to three factors:

- the directionality of the transmit and receive antennas
- the larger distances from the interferers than from the desired source
- the use of spread spectrum waveforms

We expect that the combination of these three factors (which might easily be 50 dB) will be enough to reduce interference to levels small enough even for operation in a fading environment.

3) ROUTING

A network issue arising in the system is that of routing. Specifically, if there are 4 submarines arranged as 3 at the corners of an equilateral triangle and one at the center, then it is not clear if the traffic between corner submarines should be direct, or if it should transit via the center submarine.

In the routing problem for wire networks, the links and their capacities are given, and the only issue is that of deciding the routing pattern that will minimize some network cost, like message delay. The problem at hand is very different in that delay is not an important issue, and it is the existence of the links that is questioned. As LPI is an important requirement of the system, we have attacked the routing problem from that angle.

Specifically in the next section, we will find the routing pattern that requires the least total power for a given data rate, the idea being that larger power increases the probability of detection. We will see that routing through the center is preferable, as the increase in power required at the center is made up by an even higher decrease at the corners.

That approach neglects the fact that as the data rate is increased on the link between the center and the corner, then the spread spectrum margin must be reduced if the total bandwidth is kept constant. That gives an advantage to the interceptor. However that advantage does not get close to making up for the reduction of power possible by routing through the center.

Implicit in these analyses is that the channel bandwidth is much larger than the data rate, so that signal power only increases linearly with rate for a given probability of error (the increase in rate is handled by using more dimensions in the available signal space, not by transmitting more bits per dimension).

3.1 Minimizing total power

The transmission loss (in dB) between points located at distance r can be written as

$$TL = 10 \log(e) [K (\ln r - \ln r_0) + a(f) (r - r_0)]$$

where r_0 is a reference distance, a(f) is an attenuation coefficient depending on the frequency f, and K = 0,1,2 or 3 depending on the mode of the wave spreading (none,cylindical,spherical or hyperspherical; in the open ocean it would be 2).

Consider now Figure 1. There are 3 nodes, A, B and C. There are two ways through which data can flow from A to B; either directly through a distance $r_{1,}$ or via C. The latter case corresponds to two transmissions, each over a distance of r. The transmitted power in the first case will be denoted by P_1, while P denotes the transmitted power at A and at C in the second case. There is a relationship between P_1 and P imposed by the fact that the received power P_0 at B should be the same in both cases.

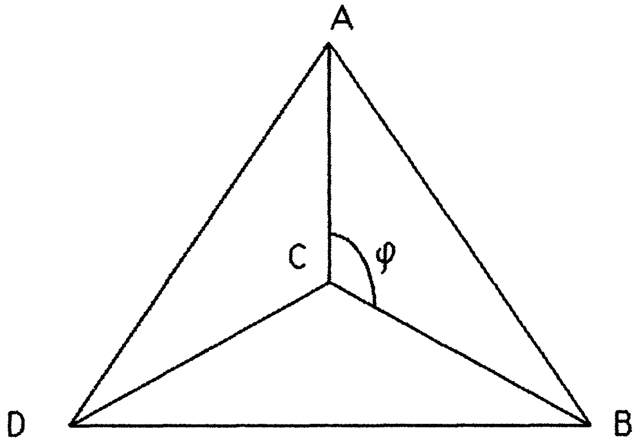

Figure 1 : platform configuration

Using the formula given above for the transmission loss we obtain:

$$\ln P_1 - \ln P = K \ln (r_1 / r) + a(f) (r_1 - r)$$

It is convenient to define the angle (ACB) as t and to note that

$$r_1/r = 2 \sin(\varphi/2)$$

The power efficiency of the double-hop routing with respect to the single-hop routing is defined naturally as

$$G(r,t) = 10 \log(e) \ln(P_1/ (2 P)) \quad \text{dB}$$

$$= 10 \log(e) [(2 \sin(\varphi/2) - 1) a(f) r + w(\varphi)]$$

where $w(\varphi) = K \ln(\sin(\varphi/2)) + (K-1) \ln(2)$ is independent of r.

That formula is plotted in Figure 2 for K=2 (open ocean).

Note that in region i) ($\varphi < \pi/3$) both $w(\varphi)$ and the coefficient of r in the formula for G(r,t) are negative, thus at acute angles double-hop routing never reduces total power.

In region ii) ($\pi/2 < \varphi < \pi$) both $w(\varphi)$ and the coefficient of r are positive, thus double-hop routing always helps.
This is the case with the triangular configuration.

Finally in region iii) ($\pi/3 < \varphi < \pi/2$) the coefficient of r is positive, but $w(\varphi)$ is negative. Thus double-hop routing reduces total power if the distance r is large enough. The value of the treshold depends on the attenuation coefficient a(f)

In conclusion, from a total power point of view double hop routing is always appropriate in the triangular configuration. The next section analyzes what happens if the reduction in spread-spectrum margin on link CB due to the increase in data rate on that link is taken into account.

Figure 2

Power Efficiency for K=2

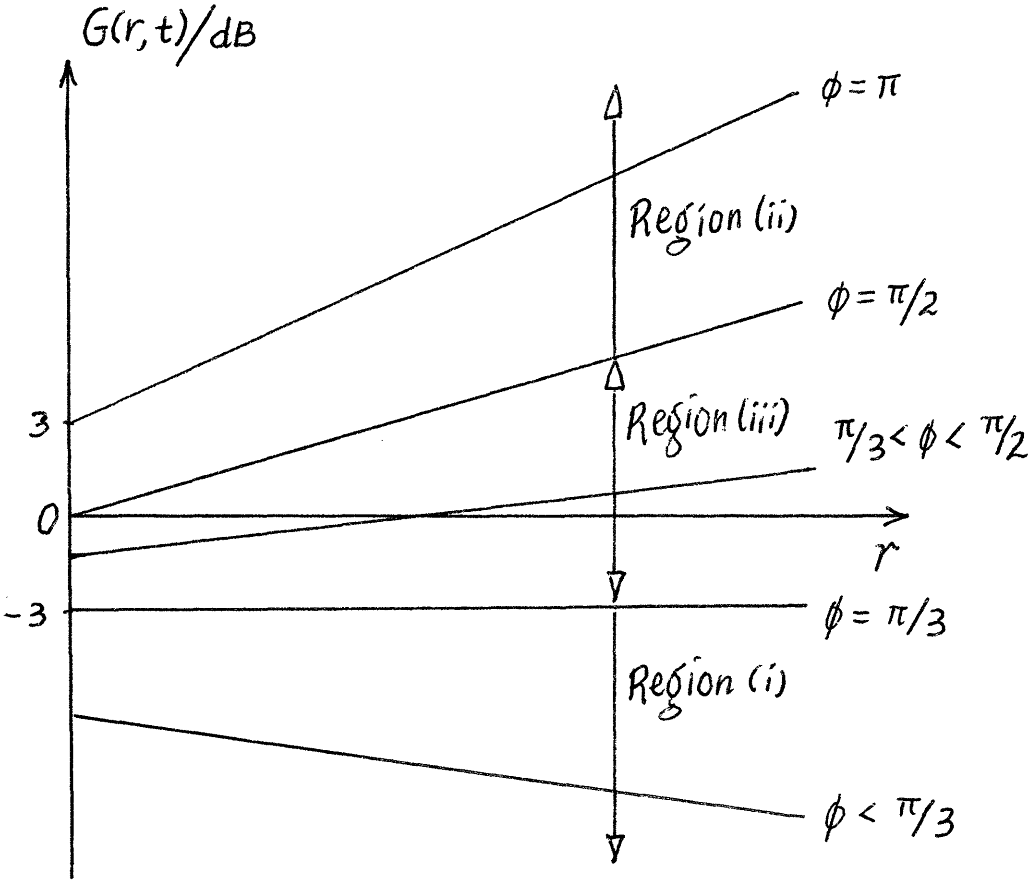

3.2. Network Routing Patterns – LPI Consideration

3.2.1. Network Configuration and routing alternatives

The expected submarine network configuration consists of 4 submarines, 3 of them at the corners of an equilateral triangle and a fourth one at the center as shown in figure 1. In this network configuration a routing issue appears: should communication between the corners of the triangle be direct, or should it be relayed through the center.

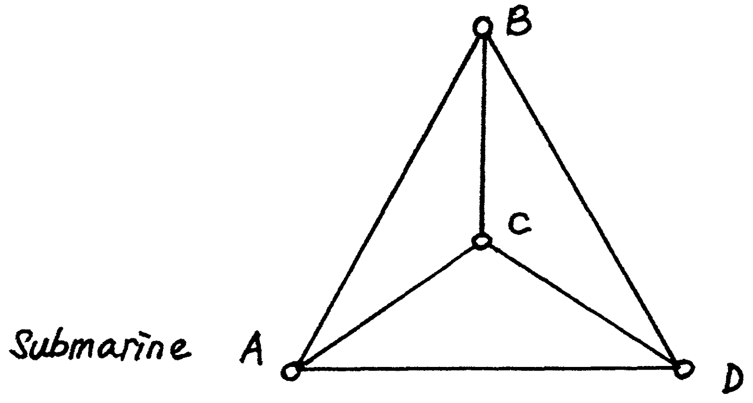

Figure 1. Network Configuration

We may simplify the problem by concentrating, without any loss of generality, only on the communications from submarines A and C to submarine B. In a direct routing situation, as shown in figure 2a, submarines A and C transmit directly to submarine B, with equal data rate R_D. In an indirect routing situation, data rate of transmission from submarines C to B is increased to $2R_D$, due to the additional traffic routed through submarine C, but originated from submarine A. The data rate from A to C is R_D.

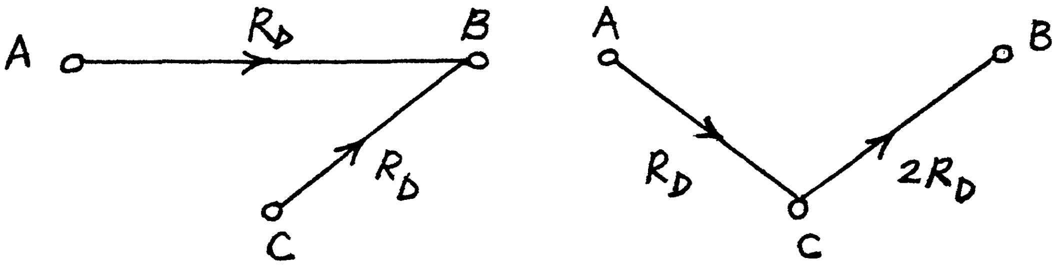

Fig 2a. Direct Routing Fig 2b. Indirect Routing

We first note that a larger power is needed to transmit over a longer distance, and if the distance between submarines A and B is larger than that between submarines A and C, then the probability for the transmission from submarine A to be intercepted is lower in the indirect routing case than that in the direct routing case. However, with the increase in data rate over the link between submarines C and B, the probability for the transmission from submarine C to be intercepted is larger in the indirect routing case than that in the direct routing case.

To study the trade-off between the two routing options in terms of the over-all probability of interception for the whole fleet of submarines, it is first necessary to know the amounts by which the probability of intercept decreases for transmission from submarine A and increases for transmission from submarine C, by going from a direct routing option to an indirect routing option. A relationship is needed to illustrate how distances and data rates affect probability of interception. This is done in the following section.

3.2.2. LPI Analysis

In the Low Probability of intercept (LPI) analysis presented here, the interceptors are assumed to be hydrophones, randomly placed over the ocean floor. Each of these hydrophones is modelled as a chip radiometer, which is a simple energy detector, over a part of the total transmission bandwidth.

By considering these hydrophones to be randomly, and uniformly, distributed over the whole ocean floor, comparison of probabilities of interception of a submarine under different routing options can be done simply by comparing the ranges over which an interceptor hydrophone could detect, for some probability of detection and false alarm, transmission from the submarine under these routing options.

As shown in figure 3, consider a transmission of data rate R_D from submarine A to submarine B, a distance r_s apart. The received carrier power C_s to noise power spectral density N_o ratio at submarine B receiver is

$$\frac{C_s}{N_o} = P_T G_{ST} \frac{G_{SR}}{T_{SR}} \frac{1}{kM} \left(\frac{\lambda}{4\pi r_S}\right)^K exp(-\alpha r_S) \qquad (1)$$

where

P_T = submarine A transmitter power (watts)
G_{ST} = gain of submarine A transmitting antenna in the direction of submarine B.
G_{SR} = gain of submarine B receive antenna to the desired signal
T_{SR} = system noise temperature of submarine B
M = submarine A to submarine B link margin
λ = wavelength of the transmitted signal
k = Boltzmann's constant = 1.38 x 10^{-23} (J/K)
K = spreading index (to be explained later)

Similarly, the received power to noise power spectral density at the hydrophone is

$$\frac{C_I}{N_o} = P_T G_{IT} \frac{G_{IR}}{T_{IR}} \frac{1}{k} (\frac{\lambda}{4\pi r_I})^K exp(-\alpha r_I) \tag{2}$$

where

r_I = interceptor range
G_{IT} = gain of submarine A transmitting antenna in the direction of the interceptor
G_{IR} = gain of the interceptor's receive antenna in the direction of submarine A
T_{IR} = system noise temperature of the interceptor

Note that a simple accounting of power levels and transmission losses, at the receiver of submarine B and at the interceptor hydrophone, has been used here to arrive at the above two equations. In general, the power level at the receiver, or hydrophone, depends on the position of the receiver relative to the line of transmission and on the orientation of the receive antenna. These are accounted for by the gain terms in the two equations.

In general, sonar transmission over a distance r_s suffers two major types of transmission losses. Firstly, loss due to spreading, accounted for by the $(\frac{\lambda}{4\pi r_S})^K$ term, where K is the spreading index and

K = 0 for no spreading
1 for cylindrical spreading
2 for spherical spreading
3 for hyperspherical spreading

and secondly, loss due to absorption, accounted for by the $exp(-\alpha r_s)$ term, where α is the absorption coefficient. The absorption coefficient is a well-tabulated parameter that depends on the temperature of the sea water, the depth of the submarines and the sonar transmit frequency.

The bit energy E_{bs} to noise power spectral density N_o at the receiver of submarine B is

$$\frac{E_{bs}}{N_o} = \frac{C_s}{N_o R_D} \tag{3}$$

where R_D is the data rate of the transmission.

From equation (1) and (3),

$$\frac{E_{bs}}{N_o} = P_T G_{ST} \frac{G_{SR}}{T_{SR}} \frac{1}{kM} \frac{1}{R_D} (\frac{\lambda}{4\pi r_S})^K exp(-\alpha r_S) \tag{4}$$

Inserting the relationship of P_T from equation (2) and (4) gives

$$\frac{C_I}{N_o} = [\frac{G_{IT}}{G_{ST}} \frac{G_{IR}}{G_{SR}} \frac{T_{SR}}{T_{IR}} M \frac{E_{bs}}{N_o}] R_D (\frac{r_S}{r_I})^K exp[\alpha(r_S - r_I)] \tag{5}$$

The effective post-detection SNR in the interceptor chip radiometer is well-known to be, in the absence of fading,

$$d = \frac{C_I}{N_o \xi} (\frac{W_I}{W}) \sqrt{\frac{T}{W_I}} \tag{6}$$

where

$\xi = 1$ for $W_I T$ products greater than 10
T = total integration time
W = total transmission bandwidth
W_I = bandwidth of interceptor receiver $\leq W$

The communication signal will be detectable for some probability of detection P_D and false alarm P_{FA}, if the interceptor's SNR exceeds some threshold value d_T. Hence at the threshold, let $d_T = d$, and from equations (5) and (6),

$$d_T = [\frac{G_{IT}}{G_{ST}} \frac{G_{IR}}{G_{SR}} \frac{T_{SR}}{T_{IR}} M \frac{E_{bs}}{N_o}] \frac{1}{\xi} R_D (\frac{W_I}{W}) \sqrt{\frac{T}{W_I}} (\frac{r_S}{r_I})^K exp[\alpha(r_S - r_I)] \tag{7}$$

By letting

$$\beta = [\frac{G_{IT}}{G_{ST}} \frac{G_{IR}}{G_{SR}} \frac{T_{SR}}{T_{IR}} \frac{M}{\xi d_T} \frac{E_{bs}}{N_o}] (\frac{1}{W}) \sqrt{W_I T} \tag{8}$$

a constant in our analysis, we now arrive at the desired equation relating r_I, the interceptor range, with r_s, the distance between the transmitter and the receiver, and R_D the transmission data rate.

$$r_I{}^K e^{\alpha r_I} = \beta R_D r_S{}^K e^{\alpha r_S} \tag{9}$$

Note that in arriving at this relationship, we have assumed that the interceptor's hydrophone listens to a fixed band of frequency W_I with integration time T.

To compare two routing options, assume that in case 1 r_s and R_D are r_1 and R_1 respectively and in case 2, r_s and R_D are changed to r_2 and R_2 respectively,

For case 1,

$$r_{I1}{}^K e^{\alpha r_{I1}} = \beta R_1 r_1{}^K e^{\alpha r_1} \tag{10}$$

For case 2,

$$r_{I2}{}^K e^{\alpha r_{I2}} = \beta R_2 r_2{}^K e^{\alpha r_2} \tag{11}$$

where r_{I1} and r_{I2} are the interceptor ranges for case 1 and case 2 respectively.

From equations (10) and (11) we have,

$$(\frac{r_{I2}}{r_{I1}})^K exp[\alpha(r_{I2} - r_{I1})] = (\frac{R_2}{R_1}) (\frac{r_2}{r_1})^K exp[\alpha(r_2 - r_1)] \tag{12}$$

Let

$$\theta = \frac{r_{I2}}{r_{I1}}$$

$$\mu = \frac{r_2}{r_1}$$

$$\rho = \frac{R_2}{R_1}$$

$$\Delta = \frac{r_{I1}}{r_1}$$

Substituting these ratios into equation (12), we have,

$$\theta^K e^{\alpha \Delta r_1 (\theta - 1)} = \rho \mu^K e^{\alpha r_1 (\mu - 1)} \tag{13}$$

This equation therefore relates θ, the proportional change in interceptor range with μ, proportional change in transmission distance, and ρ, proportional change in transmission data rate. Δ is the ratio between interceptor range and transmission distance in case 1, and depends mostly on antennas gains. As mentioned before, the interceptor range is used as a measure of the probability of interception when the transmission data rate and the distance between the transmitter and receiver change under different routing options. This equation will be analyzed in detail in the next section for trade-offs between direct and indirect routing options.

3.2.3. Numerical Results

As in figure 3, let

r = the distance between submarines A and B.
ϕ = the angle ACB

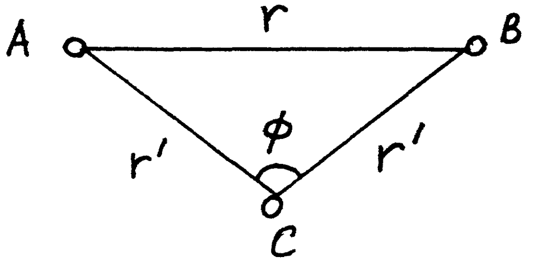

Figure 3. Network Geometry

From geometry, the distance between submarines A and C, which is equal to the distance between submarines C and B, is

$$r' = r\left[\frac{1}{2(1 - cos\phi)}\right]^{1/2} \tag{14}$$

For submarine A, there is no change in transmission data rate, hence, $\rho_A = 1$. The proportional change in transmission distance is

$$\mu_A = \frac{r'}{r} = \left[\frac{1}{2(1 - cos\phi)}\right]^{1/2} \tag{15}$$

Hence equation (13) becomes

$$\theta_A{}^K exp[\alpha\Delta r(\theta_A - 1)] = \mu_A{}^K exp[\alpha r(\mu_A - 1)] \tag{16}$$

for submarine A, where θ_A is the proportional change in interceptor range for submarine A.

For submarine C, there is no change in transmission distance, hence, $\mu_C = 1$. But the transmission data rate has doubled to give

$$\rho_C = \frac{2R_D}{R_D} = 2 \tag{17}$$

Hence equation (13), together with equation (15), gives

$$\theta_C{}^K exp[\alpha\Delta r'(\theta_C - 1)] = \rho_C \tag{18}$$

for submarine C, where θ_C is the proportional change in interceptor range for submarine C. Substituting equation (14) into (18), we have,

$$\theta_C{}^K exp[\alpha\Delta\mu_A r(\theta_C - 1)] = \rho_C \tag{19}$$

Table 1 tabulates the results of some numerical computation using equations (16) and (19). The value of α, the absorption coefficient, used is 3.5 dB/km. This is the absorption coefficient corresponding to an ocean temperature of 40° F, sonar frequency of 20 kHz at a depth of about 1/2 miles. Some other values used include K = 2, for spherical spreading, r = 15 km, and $\Delta = 10^{-2}$ for both submarines.

We first note that for $\phi \leq 60^o$, $r' \geq r$. It is obvious that indirect routing is inferior compared to direct routing in such cases. For $\phi \geq 60^o$, Table 1 tabulates the values of μ_A, θ_A and θ_C, using $\rho_C = 2$.

It is observed that for very small increase in ϕ, i.e., a very small decrease in transmission distance, the LPI performance for submarine A improves tremendously. For example, for $\phi = 95^o$, $\theta_A = 0.1$, in other words, the interceptor range for submarine A drops by some 10 folds by going from a direct to an indirect routing. This is achieved with an increase of only 39% in the interceptor range for submarine C, since $\theta_C = 1.39$. In the configuration described in figure 1, $\phi = 120^o$.

Table 2 tabulates ρ_C and θ_C for more values of ρ_C other than 2, for $\phi = 90^o$ and 120^o. It is again observed that a large amount of increase in ρ_C is needed to bring about a significant increase in θ_C.

Table 1. Numerical Computation of Eq. (16) and (19)

ϕ	μ_A	θ_A	$\theta_C(\rho_C = 2)$
60	1	1	1.385
65	0.93	0.63	1.385
70	0.87	0.42	1.385
75	0.82	0.29	1.385
80	0.78	0.21	1.39
85	0.74	0.16	1.39
90	0.71	0.13	1.39
95	0.68	0.10	1.39
100	0.65	0.085	1.39
105	0.63	0.071	1.395
110	0.61	0.061	1.395
115	0.59	0.053	1.395
120	0.58	0.048	1.395

Table 2. Effect of a Change in Data Rate On LPI Performance. From Eq. (19)

$\phi = 90^o$		$\phi = 120^o$	
ρ_C	θ_C	ρ_C	θ_C
1	1	1	1
1.5	1.21	1.5	1.22
2.0	1.4	2.0	1.40
3.0	1.68	3.0	1.7
10.0	2.91	10.0	2.96
20.0	3.94	20.0	4.00
30.0	4.68	30.0	4.80
50.0	5.75	50.0	5.95
100.0	7.56	100.0	7.87
1000.0	16.38	1000.0	17.67
10^4	29.54	10^4	32.88

3.2.4. Conclusion

It is found out that transmission distances affect LPI performance much more serverly than would transmission data rates. So it is better, when considering the network LPI requirement, to relay transmission through a nearby submarine, which in our network configuration is the submarine at the center. Indirect routing provides a better LPI performance for the whole fleet of submarines.

4) Coding and ARQ for reliable transmission and LPI

The last part of our research was devoted to the use of forward error correction (FEC) and automatic repeat request (ARQ) to provide reliable communication without using much power, thus resulting in good LPI performance. A complete analysis is attached in Appendix. It assumes that non-conherent FSK modulation is used on a Rayleigh fading channel.

Four systems are analyzed:
- plain ARQ without coding
- ARQ with Block Coding
- ARQ with Convolutional Coding
- ARQ with time diversity signaling (repetition coding)

In each system data bits are formed in groups of size n to which is appended an error detection checksum and framing overhead of size h. The resulting frame of n + h bits is passed to an encoder of rate R_c (either block or convolutional; in the case of block, the block size is K). The output of the encoder is then passed to a modulator.

At the receiver demodulation is followed by error correction. If any residual errors are detected (through the checksum) a repetition is requested.

The key performance criteria used are the detectability of the signal (called λ) and the efficiency with which the channel is used (called μ). A key variable that must be optimized on is the block size n. The key results are summarized in figure 25 of the Appendix where it is shown that using Block or Convolutional codes allow to operate with both a higher efficiency and lower detectability than using plain ARQ, even with diversity transmission. Except in the case of plain ARQ without diversity it appears to be fruitless to try to vary μ, its value at a reasonable operating pint is very much dictated by the other parameters of the system.

The Appendix considers only systems where the probabilty of undetected error is negligible. In some situations it is permissible to have many errors in the data; such situations can also be depicted on figure 25. For example the operating point for a system without FEC and ARQ has efficiency $\mu = 1$ and requires a signal to noise ratio x of 20 dB for a Probability of error of 10^{-2}; for such a value of x, λ (= μ/x^2) is 10^{-4} which is surprisingly still not as good from a LPI standpoint as using an "error free" ARQ combined with FEC. It is only for larger probability of error that dropping ARQ and FEC pays off from an LPI standpoint.

Appendix A:

ERROR CONTROL IN

LOW-PROBABILITY-OF-INTERCEPT COMMUNICATIONS

Whay Chiou Lee

ABSTRACT

The problem of error control in low-probability-of-intercept (LPI) communications is complicated by two somewhat conflicting performance objectives, namely throughput efficiency and LPI performance . Maximizing throughput calls for a high signal-to-noise ratio, whereas a high signal-to-noise ratio often leads to poor LPI performance. The trade-off between the throughput of an ideal selective repeat ARQ system and its corresponding LPI performance, based on the quality factor of an energy detector, is analyzed. The analysis assumes that the channel error probability is given. In particular, the channel error probability corresponding to a non-coherent binary FSK over a Rayleigh fading channel is used as an example. The application of FEC coding for improved system performance is investigated. ARQ systems with time diversity signaling of orders 2,4 and 8 are also studied. It is shown that, in all cases, any optimal operating point with respect to a given reward function of throughput and LPI performance lies on an Efficiency Frontier. The Efficiency Frontiers for ARQ systems with various length of the header, and those operating in fading channels with various attenuation are generated on the computer.

TABLE OF CONTENTS

LIST OF ILLUSTRATIONS

Figure Page

LIST OF THEOREMS

LIST OF TABLES

§1 INTRODUCTION

There are two basic approaches to error control, namely Forward-Error-Correction (FEC) and Automatic-Repeat-and-Request (ARQ) schemes [1]. ARQ techniques are particularly useful for low-probability-of- intercept (LPI) communications because they allow signals to be transmitted at low signal-to-noise ratios, at the expense of multiple transmissions. However, when the number of retransmissions is very large, the probability of intercept becomes considerable. The expected number of retransmissions can be reduced by improving the channel bit error probability. One way to lower the bit error probability is to use FEC coding in addition to ARQ. The error correction coding and the error detection coding in the ARQ system may be concatenated as two separate operations [2]. They may also be combined into a so called hybrid ARQ [3]. If very low error probability is not an objective *(as for non-control data here)*, then FEC can be used without ARQ for potential LPI improvement. This will not be investigated in this report.

There are many different ARQ schemes, the throughputs of which are well known [3]. In particular, the throughput of an ideal selective-repeat ARQ system *(in data bits per channel transmitted bit)* with infinite buffering is given by

$$\mu = \left(\frac{n}{n+h}\right)P_c \tag{1}$$

where n is the length of the data block in bits, h the length of the header in bits *(Including the Cyclic-Redundancy-Check bits)* ,and P_c the probability that a transmitted block contains no error. It is widely known that (1) represents an upper bound on the throughput of all ARQ systems [4].

The problem of error control in LPI communications is complicated by two somewhat conflicting performance objectives, namely throughput efficiency and LPI performance. Maximizing throughput calls for a high signal-to-noise ratio. On the contrary, a high signal-to-noise ratio often leads to poor LPI performance. There is a significant trade-off between throughput efficiency and LPI performance. The above trade-off and its implications on system design for LPI communications are discussed in subsequent sections.

The basic purpose of an LPI capability is to minimize the probability that the transmitted signals are intercepted by an adversary. In [5], several types of intercept detectors for spread-spectrum signals have been described. One common intercept detector is an energy detector. The performance of an energy detector is measured by its effective post-detection signal-to-noise ratio, d, given below [5] [6].

$$d = G\left(\frac{E_b/N_0}{W/R_D}\right)\sqrt{W_I T} \tag{2}$$

where T is the total time taken in seconds to transmit a given message, R_D the data rate in bits per second, W the bandwidth of the system in hertz, W_I the bandwidth of the interceptor in hertz, and E_b/N_0 the average energy-to-noise ratio per data bit. G is a scenario-dependent factor [6].

A signal is said to be detectable by the interceptor if

$$d \geq d_T \tag{3}$$

where d_T is the interceptor's detection threshold for given probabilities of detection and false alarm. Equivalently, a signal is detectable if

$$G \geq d_T\left(\frac{W/R_D}{E_b/N_0}\right)\sqrt{\frac{1}{W_I T}} \tag{4}$$

Note that the detection threshold is modified by the processing gain due to modulation and coding, bandspreading, as well as a factor that is inversely proportional to $\sqrt{T}$. This threshold multiplier is often known as the quality factor of the LPI system. The larger the value of this quality factor, the greater the threshold that the interceptor must exceed in order to detect the signal. Let this quality factor *(i.e. the threshold multiplier in (4))* be denoted by Q.

Suppose that the total length of the message is S bits, and the transmission rate is R encoded information bits per second. Let β be the expected number of transmissions of each communicated block. Then, the total time to transmit the message is

$$T = \beta\left(\frac{S}{n}\right)\left(\frac{n+h}{R}\right) \tag{5}$$

But, it is easy to verify that

$$\beta = P_c + 2(1-P_c)P_c + 3(1-P_c)^2 P_c + ... = \frac{1}{P_c} \tag{6}$$

Therefore,

$$T = \frac{S}{\mu R} \tag{7}$$

And, the quality factor, Q, can be written as follows.

$$Q = \left(\frac{W/R_D}{E_b/N_0}\right)\sqrt{\frac{\mu R}{W_I S}} \tag{8}$$

Let x be the average energy-to-noise ratio per ARQ bit, and R_A be the ARQ bit rate. Then,

$$(E_b/N_0)R_D = xR_A \tag{9}$$

And therefore,

$$Q = \frac{1}{x}\left(\frac{W}{R_A}\right)\sqrt{\frac{\mu R}{W_I S}} \tag{10}$$

Assuming that all the variables in (10), except for μ and x, are given, we can define a corresponding LPI performance index, λ, based on the quality factor Q.

$$\lambda = \frac{\mu}{x^2} \tag{11}$$

Note that $\sqrt{\lambda}$ is proportional to the quality factor, Q. From (1) and (11), we obtain

$$\lambda = \left(\frac{1}{x^2}\right)\left(\frac{n}{n+h}\right)P_c \tag{12}$$

In general, P_c increases monotonically with x, with a decreasing rate. It is clear from (1) and (12) that there exists no value of x that maximizes both μ and λ simultaneously.

In practice, one cannot choose an x that is arbitrarily large.

The block length, n, can also be used to control the throughput and LPI performance of the system [7] [8] [9]. Strictly speaking, n is a positive integer. However, for mathematical simplicity, let's pretend that n is a positive real number for the subsequent analysis. It is understood that in case the analysis results in an optimal n that is not an integer, it will be replaced by its closest integral neighbor. As n is usually a large number, the above treatment is not very critical.

§2 PROBLEM STATEMENT

Let's now state the problem more precisely. Figure 1 shows the block diagram of the ARQ system we are interested in. The system consists of four abstract layers of communications, namely the Physical Layer, the Modem, the Codec and the Data Link Control. In our analysis, the forward channel in the Physical Layer is assumed to be a Rayleigh fading channel. The analytical results can readily be modified for other channels of interest. Suppose that non-coherent binary frequency-shift-keying (FSK) is used. Then, the channel bit-error-probability is given below [10],

$$p(x) = \frac{1}{2 + \rho R_c x} \tag{13}$$

where R_c is the FEC code rate *($R_c = 1$ if FEC is not used)*, and ρ is the expected value of the square of the attenuation factor associated with the fading channel. Other modulation schemes are considered in section 4.3.

Throughout this report, we assume that the Codec is separated from its adjacent layers. ARQ systems with joint coding and modulation schemes or with hybrids of Codec and Data Link Control are beyond the scope of this work. The sending and receiving terminals perform the usual functions of a Data Link Control. The feedback channel is assumed to be error-free. This can be achieved by using appropriate link level protocols.

The design objective is to jointly maximize μ and λ, with respect to x and n, subject to some practical constraints on the control variables, and possibly a reward function of μ and λ. If the constraints and the reward function are all known, the problem is just a fairly straight-forward constrained optimization problem with multiple objectives. Suppose they are not given. Let's take a look at the set of all feasible pairs of μ and λ, for all practical combinations of x and n. It will be shown in the analysis that only a subset of these pairs are potential optimal operating points. We will discover that this subset of operating points lie on a curve which dictates the trade-off between the throughput and LPI performance of the ARQ system. In addition, this curve varies with different values of ρ and the length of the header.

Figure 1

SYSTEM BLOCK DIAGRAM

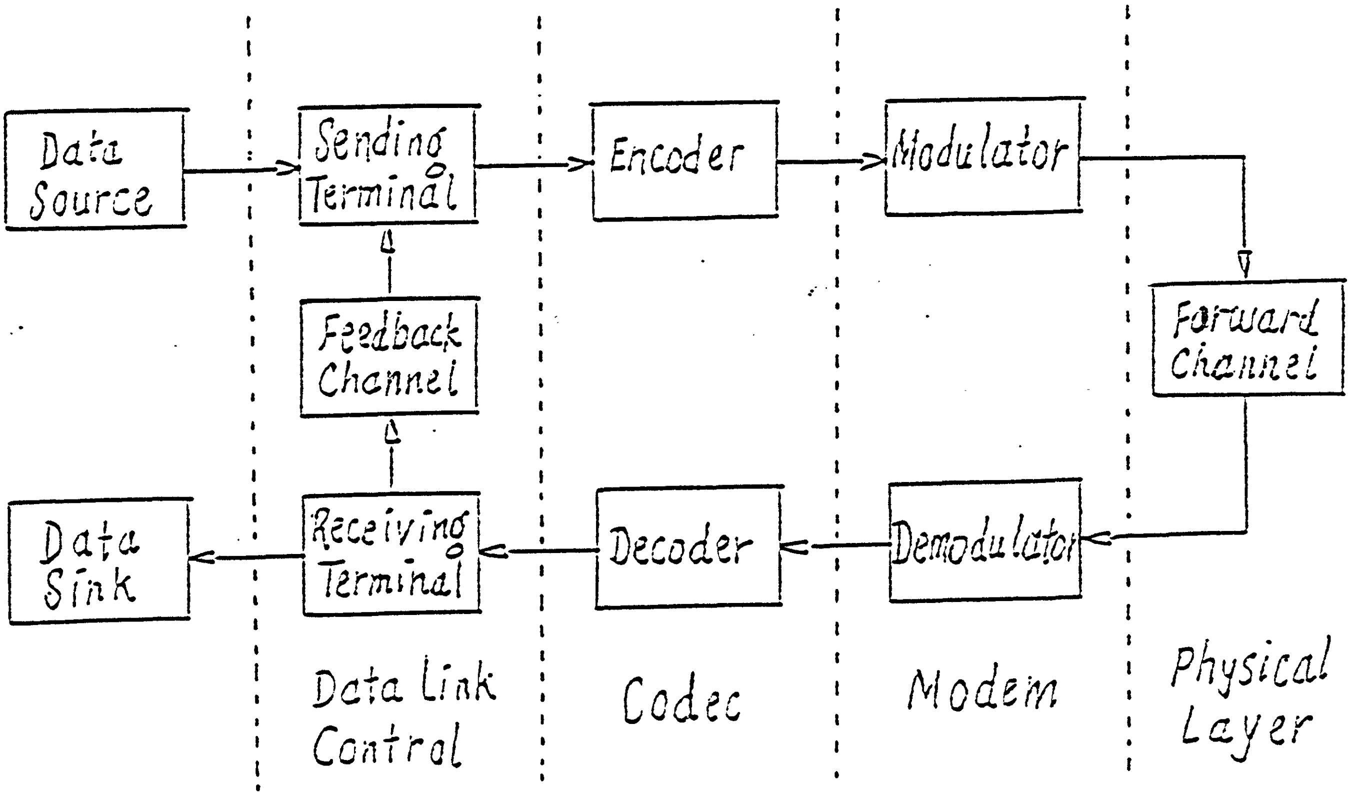

§3 ANALYSIS

We first consider the plain ARQ system. The general results are mostly applicable to the cases with FEC coding, and those with time diversity signaling, all of which will be considered in subsequent sections.

3.1 PLAIN ARQ

With neither FEC coding nor diversity signaling, $R_c = 1$, and the probability that a transmitted block contains no error is

$$P_c = \left(1 - p(x)\right)^{(n+h)} \tag{14}$$

where

$$p(x) = \frac{1}{2 + \rho x} \tag{15}$$

This assumes that errors are independent. This is true for many channels, but may not be entirely realistic for a fading channel, except when frequency hopping and interleaving are employed.

The throughput and the LPI performance index are respectively

$$\mu = \mu(x,n) = \left(\frac{n}{n+h}\right)\left(1 - p(x)\right)^{(n+h)} \tag{16}$$

$$\lambda = \lambda(x,n) = \left(\frac{1}{x^2}\right)\left(\frac{n}{n+h}\right)\left(1 - p(x)\right)^{(n+h)} \tag{17}$$

Let (x_μ^*, n_μ^*) be the pair of control variables that maximizes μ, and $(x_\lambda^*, n_\lambda^*)$ be the pair that maximizes λ. It is obvious from (15) and (16) that for $x \leq \overline{x}$,

$$x_\mu^* = \overline{x} \tag{18}$$

To determine n_μ^*, we take the derivative of μ with respect to n, and set that to zero.

$$\left.\frac{\partial \mu}{\partial n}\right|_{n^*} = \left[\frac{h}{n}\left(\frac{1}{n+h}\right) + \ln\left(1 - p(x)\right)\right]\mu\Big|_{n^*} = 0 \tag{19}$$

Thus,

$$n^*(x) = \frac{h}{2}\left\{-1 + \sqrt{1 - \left[\frac{4}{h\ln(1-p(x))}\right]}\right\} \tag{20}$$

Also,

$$\left.\frac{\partial^2\mu}{\partial n^2}\right|_{n^*} = -\left[\frac{h}{n}\left(\frac{1}{n+h}\right)^2\left(2n+h\right)\right]\mu\Big|_{n^*} < 0 \tag{21}$$

Hence, $n^*(x)$ maximizes μ for the given value of x. It follows that

$$n^*_\mu = n^*(\overline{x}) \tag{22}$$

And, the highest achievable throughput is

$$\mu_{max} = \mu(x^*_\mu, n^*_\mu) \tag{23}$$

Since λ is directly proportional to μ, with a multiplier that depends only on x, it is clear that

$$n^*_\lambda = n^*(x^*_\lambda) \tag{24}$$

Maximizing λ with respect to x, we have

$$\left.\frac{\partial\lambda}{\partial x}\right|_{x^*} = -\left\{\frac{2}{x} + (n+h)\left[\frac{1}{1-p(x)}\right]\frac{dp}{dx}\right\}\lambda\Big|_{x^*} = 0 \tag{25}$$

Hence, $x^*(n)$ satisfies

$$-\left[\frac{x}{p(x)}\left(\frac{dp}{dx}\right)\right]\Big|_{x^*} = \left(\frac{2}{n+h}\right)\left[\frac{1-p(x)}{p(x)}\right]\Big|_{x^*}. \tag{26}$$

From (15) and (26), we obtain

$$(n+h)\rho x - 2(1+\rho x)(2+\rho x)|_{x^*} = 0 \tag{27}$$

In general, there are two roots to the above quadratic equation in x. Consider the second derivative of λ with respect to x.

$$\left.\frac{\partial^2\lambda}{\partial x^2}\right|_{x^*} = -\left(\frac{2}{x^2}\right)\left[\frac{1}{(1+\rho x)(2+\rho x)}\right]\left[(\rho x)^2 - 2\right]\lambda\Big|_{x^*} \tag{28}$$

Thus, λ achieves a maximum at x^* if

$$(\rho x^*)^2 > 2 \tag{29}$$

From (27), we have

$$x^*(n) = \frac{1}{4\rho}\left(n+h-6\right)\left[1+\sqrt{1-\frac{32}{(n+h-6)^2}}\right] \tag{30}$$

Note that $\lambda(x^*(n), n)$ is a local maximum. The global maximum is infinity at $x = 0$. There is a local minimum between $x = 0$ and $x = \sqrt{2}/\rho$, where ρ is in the order of 1. Several things break down in our expression for λ when x is betwen 0 and $\sqrt{2}/\rho$. First of all, the expression for $p(x)$ breaks down over this range of x. Also, (1), which relates μ to the block error probability, breaks down. Thus, over the region of interest, $\lambda(x^*(n), n)$ is the only achievable maximum for a given value of n.

Figure 2 shows the LPI performance as a function of x for $n = 32$ and $n = 80$. In this and all subsequent examples, unless otherwise stated, h and ρ are assumed to be equal to 32 and 1 respectively.

Figure 2

LPI PERFORMANCE FOR PLAIN ARQ

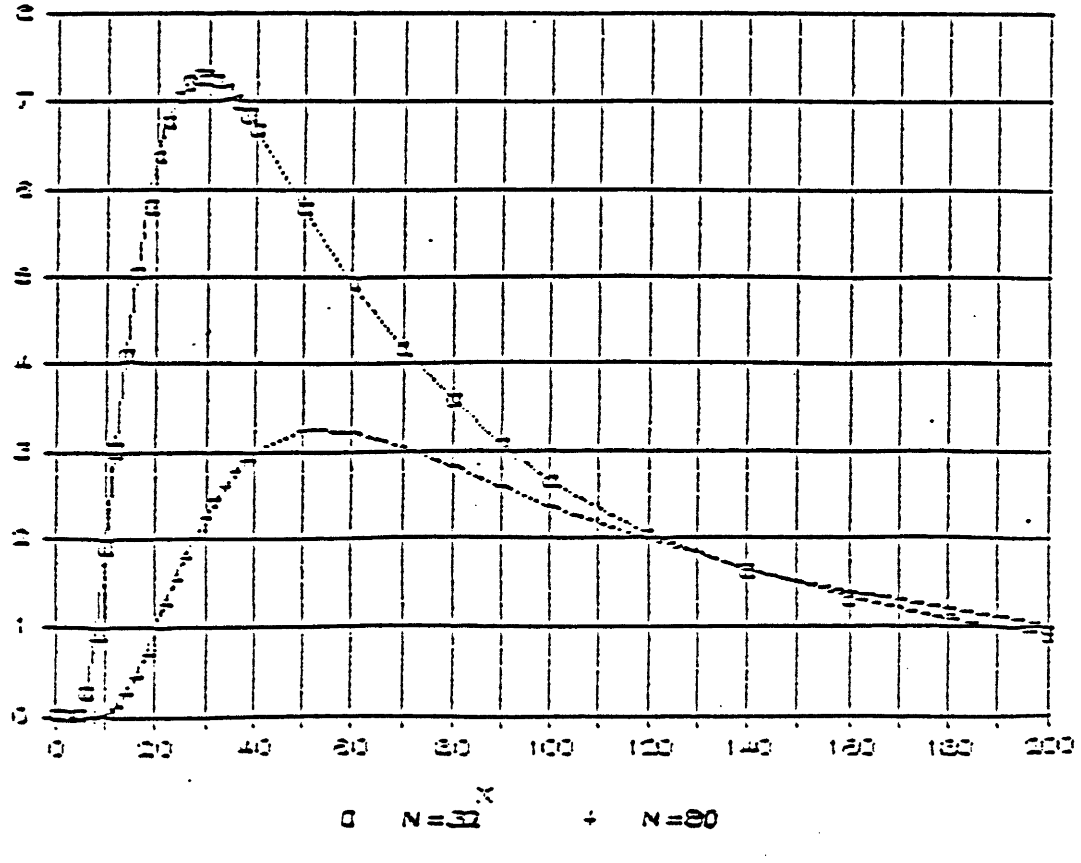

The bounds defined by (37) is shown in Figure 4. Note that $(x_\lambda^*, n_\lambda^*)$ is very close to a corner of the bounding region. It appears that this corner point is an excellent approximation of $(x_\lambda^*, n_\lambda^*)$.

Let the above approximation of $(x_\lambda^*, n_\lambda^*)$ be $(\hat{x}_\lambda^*, \hat{n}_\lambda^*)$. It can be obtained by solving the following simultaneous equations.

$$n = (2\rho x + 6 - h) \tag{48}$$

$$n = \frac{h}{2}\left(\frac{\rho x}{1+\rho x}\right) \tag{49}$$

Thus, for $h = 32$ and $\rho = 1$,

$$\hat{x}_\lambda^* = \frac{1}{\rho}\left(\frac{3h-6}{8}\right)\left\{1 + \sqrt{1 + \frac{32(h-6)}{(3h-16)^2}}\right\} = 20.6 \tag{50}$$

$$\hat{n}_\lambda^* = (2\rho\hat{x}_\lambda^* + 6 - h) \approx 15 \tag{51}$$

Recall that $(x_\lambda^*, n_\lambda^*) = (20.4, 15)$. Hence, $(\hat{x}_\lambda^*, \hat{n}_\lambda^*)$ is indeed a very good approximation.

Even though (50) and (51) are explicit functions of h it is not immediately transparent how $\hat{x}_\lambda^*$ and $\hat{n}_\lambda^*$ vary with h. It will be even less transparent if (50) and (51) are used to derive approximations for $\mu_{\lambda_{max}}$ and λ_{max}.

From (37), we see that n_λ^* is upper bounded by $h/2$. We now show that n_λ^* is well approximated by

$$\hat{n}_\lambda = \frac{h}{2} = 16 \tag{52}$$

Figure 4

BOUNDS ON $(x_\lambda^*, n_\lambda^*)$ FOR PLAIN ARQ

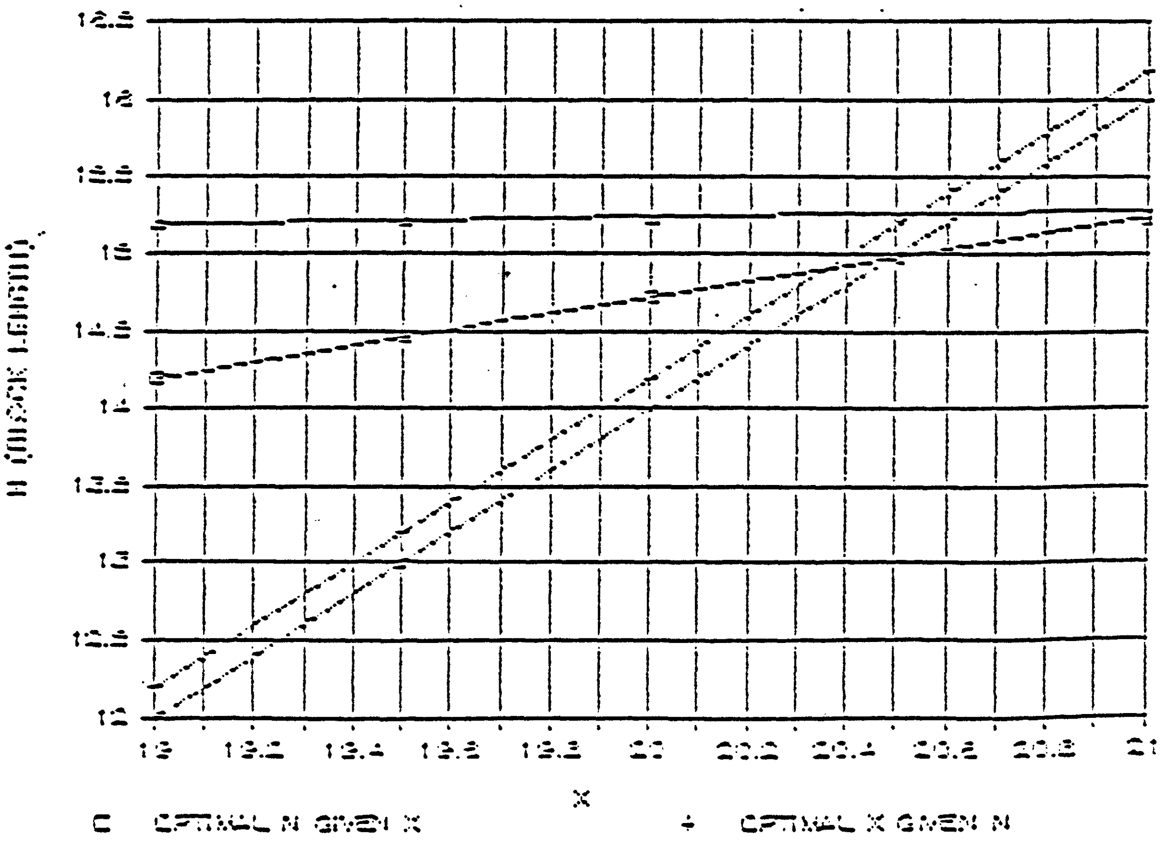

Theorem 1.1

An approximation for n_λ^* is given by

$$\hat{n}_\lambda = \left(\frac{h}{2}\right) \tag{53}$$

Proof of Theorem 1.1

From (30), we obtain the following lower bound on x_λ^*.

$$x_\lambda^* \geq \frac{1}{4\rho}\left(n_\lambda^* + h - 6\right) \geq \frac{1}{4\rho}\left(h - 6\right) \tag{54}$$

It follows from (15) and (54) that

$$p(x_\lambda^*) \leq \left(\frac{4}{h+2}\right) \ll 1 \tag{55}$$

Thus, $p(x_\lambda^*)$ tends to zero with increasing value of h.

From (15) and (44), we have

$$\lim_{p(x)\to 0}\{w(x)\} = \lim_{p\to 0}(1-2p) = 1 \tag{56}$$

It can be verified that

$$\lim_{p\to 0}\left\{\frac{p}{-(1-p)\ln(1-p)}\right\} = 1 \tag{57}$$

From (41), (56) and (57), we obtain

$$\lim_{p\to 0}\{n\} = \left(\frac{h}{2}\right) \tag{58}$$

For $x_\lambda^* \gg 2/\rho$, and any practical value of h, $p(x_\lambda^*) \ll 1$. Hence, (53) is a good approximation for n_λ^*.

Q.E.D.

We can similarly find good approximations for x_λ^*, $\mu_{\lambda_{max}}$ and λ_{max} respectively.

Theorem 1.2

An approximation for x^*_λ is given by

$$\hat{x}_\lambda = \frac{3}{4\rho}\Big(h - 4\Big) \tag{59}$$

Proof of Theorem 1.2

From (30), (37) and (52), we have

$$x^*_\lambda \leq \frac{1}{4\rho}\Big(\hat{n}_\lambda + h - 6\Big)\left\{1 + \sqrt{1 - \frac{32}{(\hat{n}_\lambda + h - 6)^2}}\right\} \tag{60}$$

The following bound on x^*_λ is tight for $h \gg 8$.

$$x^*_\lambda \leq \frac{1}{2\rho}\Big(\hat{n}_\lambda + h - 6\Big) = \frac{3}{4\rho}\Big(h - 4\Big) \tag{61}$$

Hence, (59) is a good approximation for x^*_λ.

Q.E.D.

Corollary 1

From (15) and Theorem 1.2, we have

$$p(x^*_\lambda) = \frac{1}{2 + \rho x^*_\lambda} \approx \frac{1}{2 + \rho \hat{x}_\lambda} \tag{62}$$

And, $p(x^*_\lambda)$ is well approximated by $\hat{p}_\lambda$ given below.

$$\hat{p}_\lambda = \frac{4}{3h - 4} \tag{63}$$

Theorem 1.3

For $h \gg 8$, $\mu_{\lambda_{max}}$ and λ_{max} are well approximated by $\hat{\mu}$ and $\hat{\lambda}$ respectively given below.

$$\hat{\mu} = \frac{1}{3}\left(\frac{3h-8}{3h-4}\right)^{3h/2} \approx \frac{1}{3e^2} \ll \frac{1}{3} \tag{64}$$

$$\hat{\lambda} = \frac{1}{3}\left(\frac{3h-8}{3h-4}\right)^{3h/2}\left(\frac{4\rho}{3h-12}\right)^2 \approx \frac{16}{27}\left(\frac{\rho}{eh}\right)^2 \tag{65}$$

Proof of Theorem 1.3

The proof follows from (16),(17),(52),(59),(63) and a well-known fact that $\lim_{t\to 0}(1+t)^{1/t} = e$.

Q.E.D.

We conclude from the above Theorems that both x^*_λ and n^*_λ increase approximately linearly with h. The approximations in (64) and (65), plotted against $\log_2(h)$, are shown in Figures 5 and 6 respectively. The locus of the point, $(\mu_{\lambda_{max}}, \lambda_{max})$, for various values of h is shown in Figure 7. Taking into consideration that the approximations are good for $h \gg 8$, we can expect that λ_{max} decreases with the length of the header while $\mu_{\lambda_{max}}$ depends only slightly on it.

The true values and corresponding approximations for x_λ^*, n_λ^*, $\mu_{\lambda_{max}}$ and λ_{max} are summarized in Table 1 for comparison. Evidently, the approximations are very good.

Table 1

Results for Plain ARQ			
x_λ^*	20.4	$\hat{x}_\lambda$	21
n_λ^*	15	$\hat{n}_\lambda$	16
$\mu_{\lambda_{max}}$	0.0373	$\hat{\mu}$	0.0395
λ_{max}	$8.96 * 10^{-5}$	$\hat{\lambda}$	$8.95 * 10^{-5}$

Figure 5

APPROXIMATE $\mu_{\lambda_{max}}$ FOR PLAIN ARQ

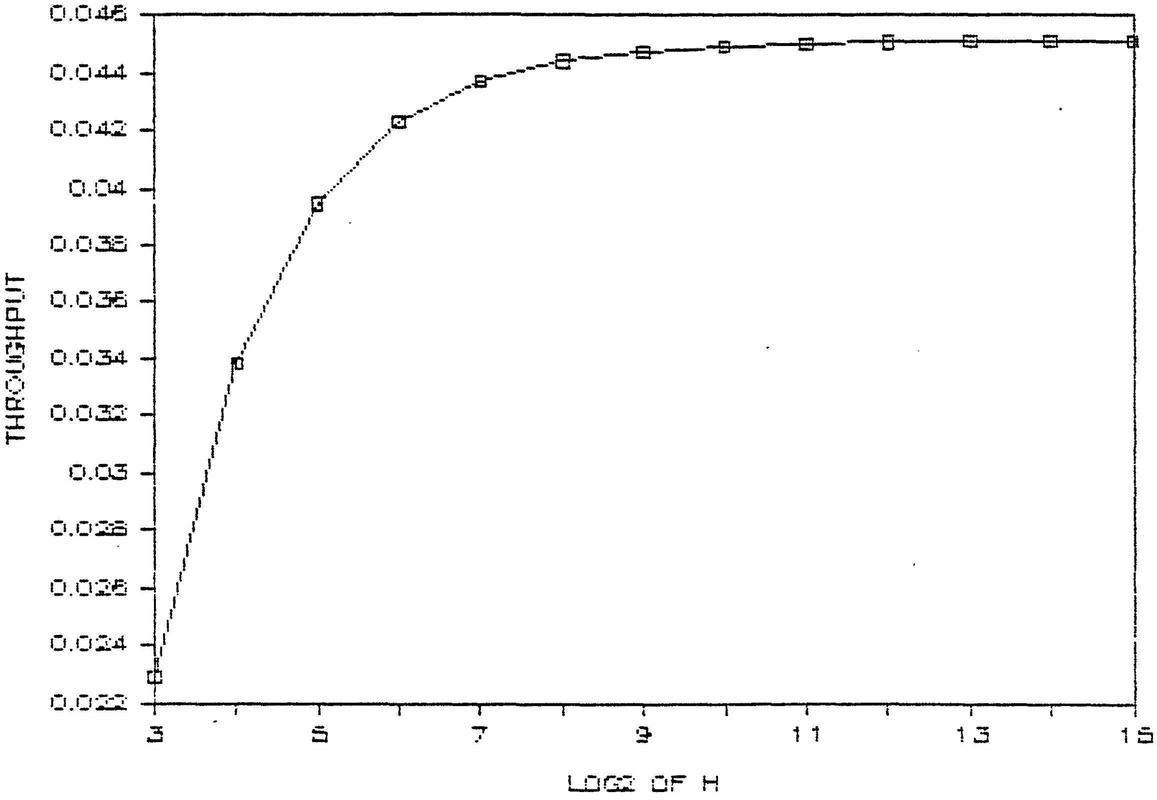

Figure 6

APPROXIMATE λ_{max} FOR PLAIN ARQ

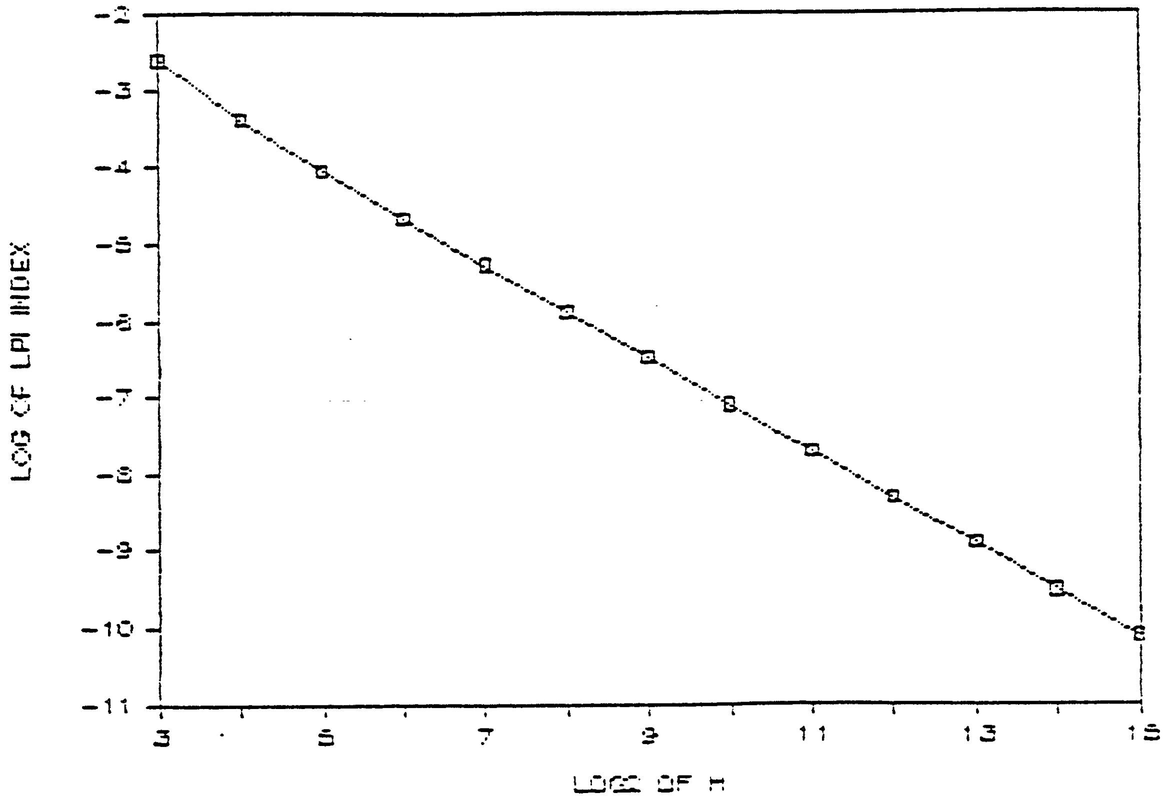

Figure 7

APPROXIMATE LOCUS OF $(\mu_{\lambda_{max}}, \lambda_{max})$ FOR PLAIN ARQ

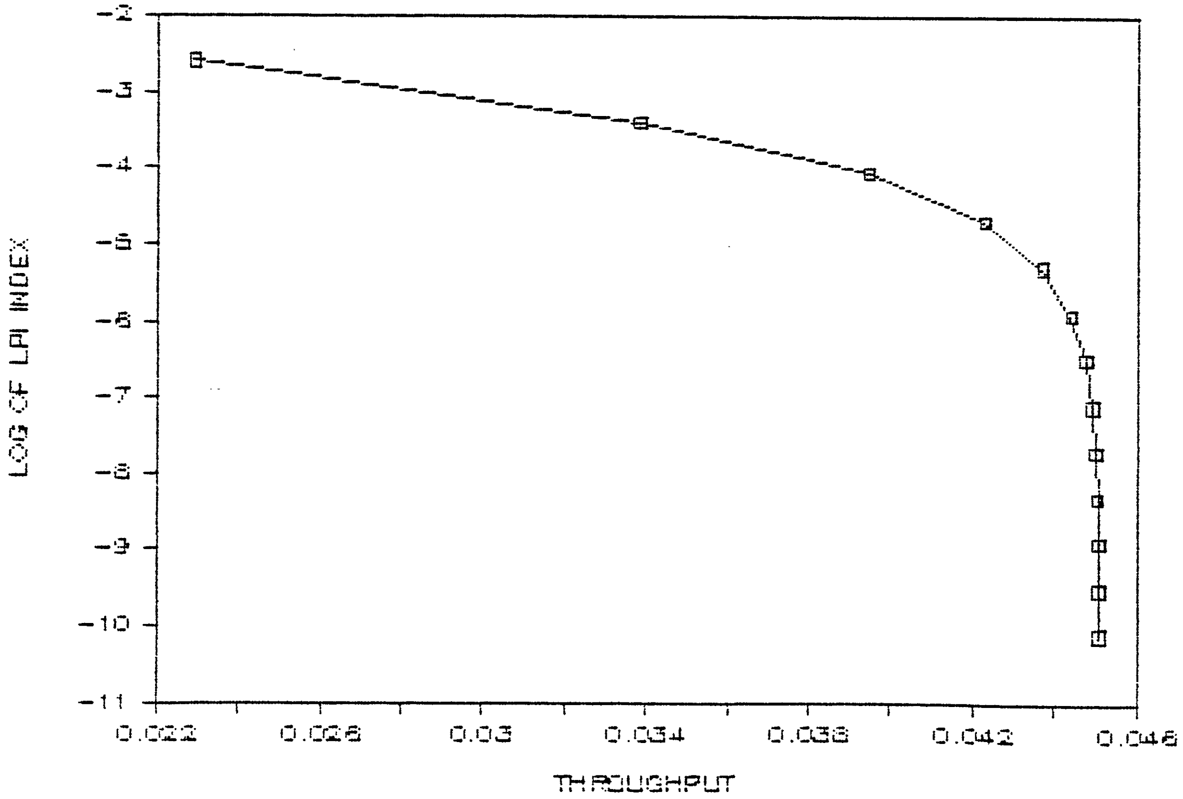

We have so far obtained two operating points, namely $(\mu_{max}, \lambda_{\mu_{max}})$ and $(\mu_{\lambda_{max}}, \lambda_{max})$. When neither throughput nor LPI performance dominates the overall system design objectives, these operating points may not be optimal. We now show that all the potential optimal operating points belong to a small subset, known as the Efficiency Frontier.

Recall that

$$\lambda = \left(\frac{1}{x^2}\right)\mu \tag{66}$$

With a fixed value of x, λ varies linearly with μ for different values of n. Figure 8 shows a family of Iso-x lines. The tip of each Iso-x line corresponds to the operating point with $\mu = \mu(x, n^*(x))$ and $\lambda = \lambda(x, n^*(x))$. For a fixed value of n, one can also vary x to trace out an Iso-n curve. As pointed out earlier, we ignore the range of x up to $\sqrt{2}/\rho$ since our model breaks down over this range. Figure 9 shows a family of Iso-n curves.

In Figure 10, the two families of curves are put together. For obvious reasons, the envelope joining A, B and C is called the Efficiency Frontier. Any point that is not on this frontier is not efficient because one can increase either μ or λ without decreasing the other. The Efficiency Frontier describes the trade-off between throughput and LPI performance. It is easily obtained by joining the tips of all the Iso-x lines for x between x_λ^* and $\bar{x}$.

A civilian user who cares only about throughput will operate at point C. When LPI performance is the primary concern, point A is the optimal operating point. Suppose that the reward function of μ and λ is

$$J(\mu, \lambda) = \min(\theta\mu, \lambda) \tag{67}$$

where $\theta \geq 0$ and increasing θ indicates increasing LPI performance requirement relative to throughput efficiency. Then, point B, as shown in Figure 10, is the optimal operating point.

The Efficiency Frontier for the plain ARQ system is shown in Figure 11. It clearly shows that good LPI performance can be achieved at the expense of throughput efficiency.

Figure 8

ISO-X LINES

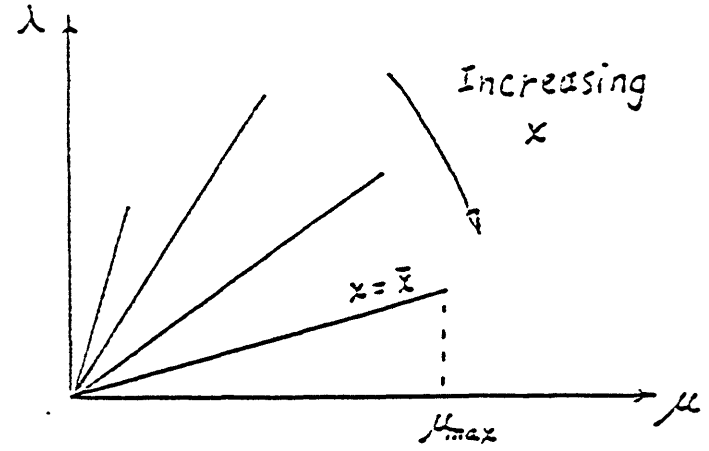

Figure 9

ISO-N CURVES

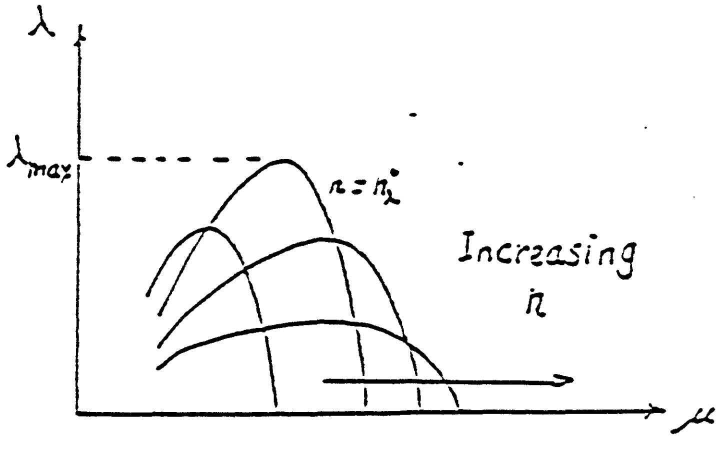

Figure 10

TRADE-OFF BETWEEN THROUGHPUT & LPI PERFORMANCE

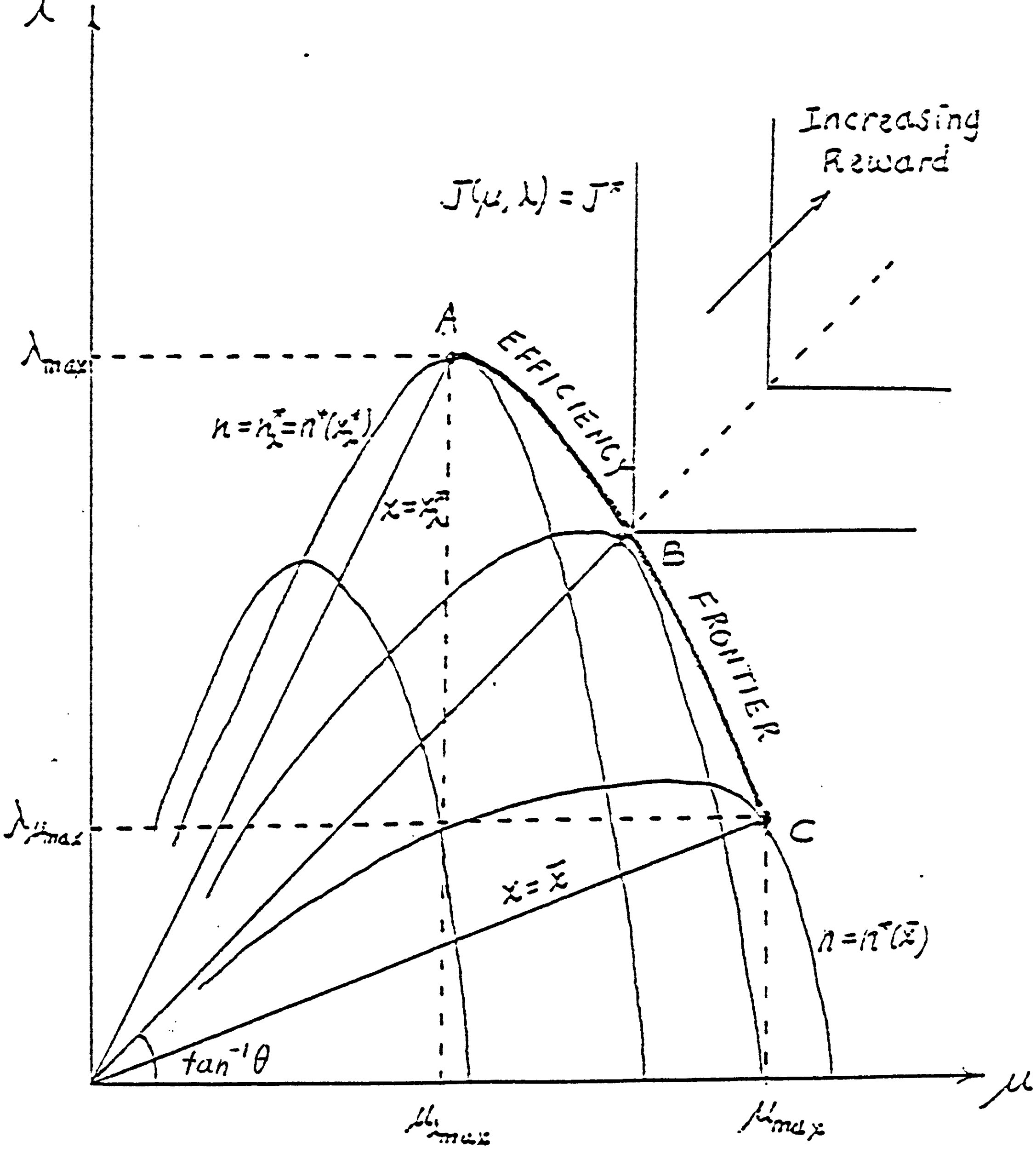

Figure 11

THE EFFICIENCY FRONTIER FOR PLAIN ARQ

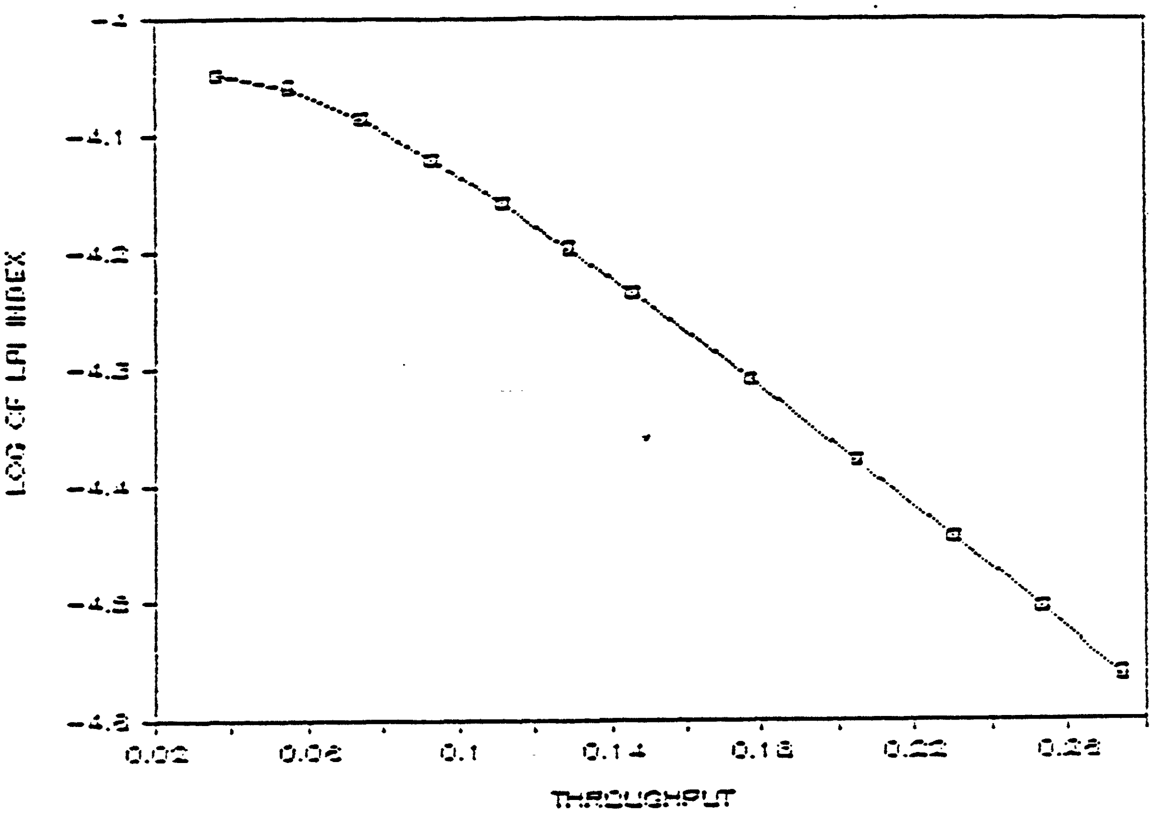

3.2 ARQ WITH BLOCK CODING

We have learned that without FEC coding, one cannot simultaneously achieve a good LPI performance and any reasonable throughput. We now consider the case with block coding.

The block diagram in Figure 1 is still applicable. The encoder receives ARQ blocks of $(n+h)$ bits, divides them into FEC blocks of K bits, and then encodes them at a rate of R_c. In this case, the probability that an ARQ block contains no error is given by

$$P_c = \left(1 - \xi(x)\right)^{(n+h)/K} \tag{68}$$

where $\xi(x)$ denotes the FEC block error probability. The throughput efficiency and LPI index are respectively

$$\mu = R_c\left(\frac{n}{n+h}\right)\left(1 - \xi(x)\right)^{(n+h)/K} \tag{69}$$

$$\lambda = \left(\frac{1}{x^2}\right)R_c\left(\frac{n}{n+h}\right)\left(1 - \xi(x)\right)^{(n+h)/K} \tag{70}$$

We can also go through a similar analysis as before, and obtain the following results.

(a) $\mu_{max} = \mu(x_\mu^*, n_\mu^*) = \mu(\overline{x}, n^*(\overline{x}))$

(b) $\lambda_{max} = \lambda(x_\lambda^*, n_\lambda^*)$ where $(x_\lambda^*, n_\lambda^*)$ solves the simultaneous equations,

$$n = n^*(x) \quad \text{and} \quad x = x^*(n)$$

(c)

$$n^*(x) = \frac{h}{2}\left\{-1 + \sqrt{1 - \left[\frac{4K}{h\ln\left(1 - \xi(x)\right)}\right]}\right\} \tag{71}$$

(d) $x^*(n)$ satisfies

$$-\left[\frac{x}{\xi(x)}\left(\frac{d\xi}{dx}\right)\right]\Bigg|_{x^*} = \left(\frac{2K}{n+h}\right)\left[\frac{1-\xi(x)}{\xi(x)}\right]\Bigg|_{x^*} \tag{72}$$

(e) $\lambda_{\mu_{max}} = \lambda(x_\mu^*, n_\mu^*)$

(f) $\mu_{\lambda_{max}} = \mu(x^*_\lambda, n^*_\lambda)$

Lemma 2

An upper bound on n^*_λ is given by

$$n^*_\lambda \leq h\left\{\frac{1}{2}w(x)\left[\frac{1}{1-\xi(x)}\right]\right\}\Bigg|_{x^*_\lambda} \tag{73}$$

where

$$w(x) = -\left[\frac{x}{\xi(x)}\left(\frac{d\xi}{dx}\right)\right] \tag{74}$$

Proof of Lemma 2

The proof follows from the steps outlined in (38) through (43) in the proof of Lemma 1.

Q.E.D.

In general, there is no closed form expression for $\xi(x)$. We will approximate $\xi(x)$ by an upper bound. Suppose that soft-decision decoding is used on a Rayleigh fading channel. Then, the block error probability for any linear block code is upper bounded as follows [10].

$$\xi(x) \leq \sum_{d=d_{min}}^{L} N_d \binom{2d-1}{d} \Big(p(x)\Big)^d = \hat{\xi}(x) \tag{75}$$

where $L = (K/R_c)$, N_d is the number of codewords with weight d, d_{min} is the minimum weight of the chosen block code, and

$$p(x) = \frac{1}{2 + \rho R_c x} \tag{76}$$

is the bit error probability for the channel.

Using $\hat{\xi}(x)$ as an approximation to $\xi(x)$, we obtain an approximation of $w(x)$, which is given below.

$$\hat{w}(x) = \frac{g(x)}{\hat{\xi}(x)} \left(\frac{\rho R_c x}{2 + \rho R_c x} \right) \tag{77}$$

where

$$g(x) = \sum_{d=d_{min}}^{L} d N_d \binom{2d-1}{d} \Big(p(x)\Big)^d \tag{78}$$

The bound in (73) becomes

$$n_\lambda^* \leq h \left\{ \frac{1}{2} g(x) \left[\frac{1}{\hat{\xi}(x)(1 - \hat{\xi}(x))} \right] \left(\frac{\rho R_c x}{2 + \rho R_c x} \right) \right\} \Bigg|_{x_\lambda^*} \tag{79}$$

Note that

$$\frac{g(x)}{\hat{\xi}(x)} \geq d_{min} \tag{80}$$

In the practical range of x, the bound in (80) is tight. And, from (77) and (80)

$$\hat{w}(x) \geq d_{min} \left(\frac{\rho R_c x}{2 + \rho R_c x} \right) \approx d_{min} \tag{81}$$

Theorem 2.1

An approximation for n^*_λ is given by

$$\hat{n}_\lambda = h\left(\frac{d_{min}}{2}\right) \tag{82}$$

Proof of Theorem 2.1

For $x^*_\lambda \gg 2/(\rho R_c)$, $\hat{\xi}(x^*_\lambda) \ll 1$. The proof then follows from (73) and (81).

Q.E.D.

Theorem 2.2

An approximation for x^*_λ is given by

$$\hat{x}_\lambda = \xi^{-1}(\hat{\xi}_\lambda) \tag{83}$$

where $\xi^{-1}(*)$ stands for the inverse of the function $\xi(*)$, and

$$\hat{\xi}_\lambda = \left\{\frac{4K}{h(d_{min}+2)d_{min}+4K}\right\} \tag{84}$$

is an approximation for $\xi(x^*_\lambda)$.

Proof of Theorem 2.2

The proof follows from (72), (74) and (81), using $\hat{n}_\lambda$ in place of n^*_λ.

Q.E.D.

Theorem 2.3

$\mu_{\lambda_{max}}$ and λ_{max} are well approximated by $\hat{\mu}$ and $\hat{\lambda}$ respectively given below.

$$\hat{\mu} = R_c\left(\frac{d_{min}}{d_{min}+2}\right)\left\{\frac{h(d_{min}+2)d_{min}}{h(d_{min}+2)d_{min}+4K}\right\}^{(d_{min}+2)h/(2K)} \ll R_c\left(\frac{d_{min}}{d_{min}+2}\right) \tag{85}$$

$$\hat{\lambda} = \hat{\mu}\left\{\xi^{-1}\left[\frac{4K}{h(d_{min}+2)d_{min}+4K}\right]\right\}^{-2} \tag{86}$$

Proof of Theorem 2.3

The proof follows from (69), (70), (82), (83) and (84).

Q.E.D.

Let's consider the Golay(24,12) block code as an example. The set of values of d, N_d, and $\binom{2d-1}{d}$ are shown in Table 2 [10].

Table 2

Golay(24,12) Block Code		
d	N_d	$\binom{2d-1}{d}$
0	1	1
8	759	6435
12	2576	$1.4 * 10^6$
16	759	$3.0 * 10^8$
24	1	$1.6 * 10^{13}$

Figure 12 shows the intersection of the two curves, $n^*(x)$ and $x^*(n)$, for $h = 32$ and $\rho = 1$. The upper bound on n^*_λ is also shown in the same figure. The true values and corresponding approximations for x^*_λ, n^*_λ, $\mu_{\lambda_{max}}$ and λ_{max} are summarized in Table 3.

Table 3

Results for ARQ with Golay(24,12) Block Code			
x^*_λ	17.6	$\hat{x}_\lambda$	16.5
n^*_λ	105	$\hat{n}_\lambda$	128
$\mu_{\lambda_{max}}$	0.2820	$\hat{\mu}$	0.3122
λ_{max}	$9.10 * 10^{-4}$	$\hat{\lambda}$	$11.47 * 10^{-5}$

Suppose that $\bar{x} = 40$. Then, we have $(x^*_\mu, n^*_\mu) = (40, 2058)$. And,

$$\mu_{max} = 0.4847 \tag{87}$$

$$\lambda_{\mu_{max}} = 3.02 * 10^{-4} \tag{88}$$

Comparing these results with those for the case without FEC coding *(See (33),(34),(35) and (36))*, we find that the Golay(24,12) block code improves the system performance by an order of magnitude. Figure 13 shows the Efficiency Frontier for the case with Golay(24,12) block code.

Figure 12

$(x_\lambda^*, n_\lambda^*)$ FOR ARQ WITH GOLAY(24,12) BLOCK CODE

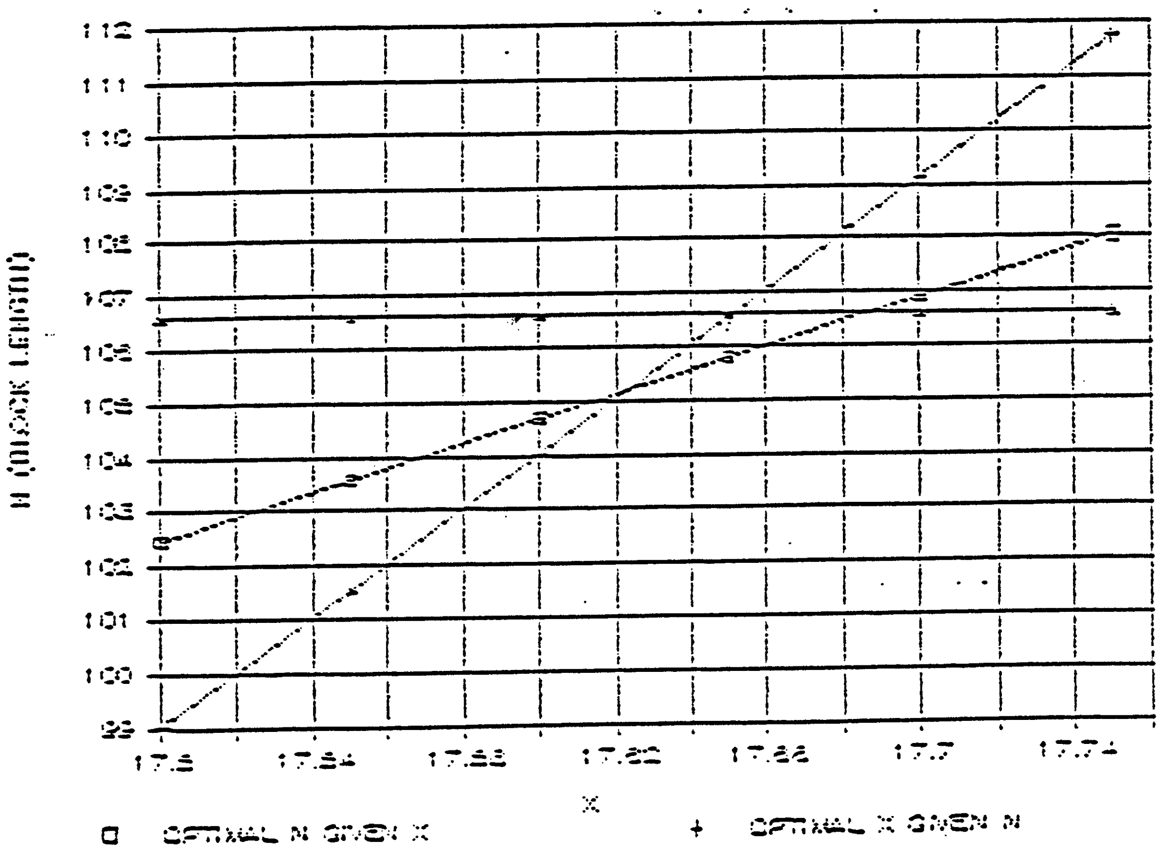

Figure 13

THE EFFICIENCY FRONTIER FOR ARQ WITH GOLAY(24,12) BLOCK CODE

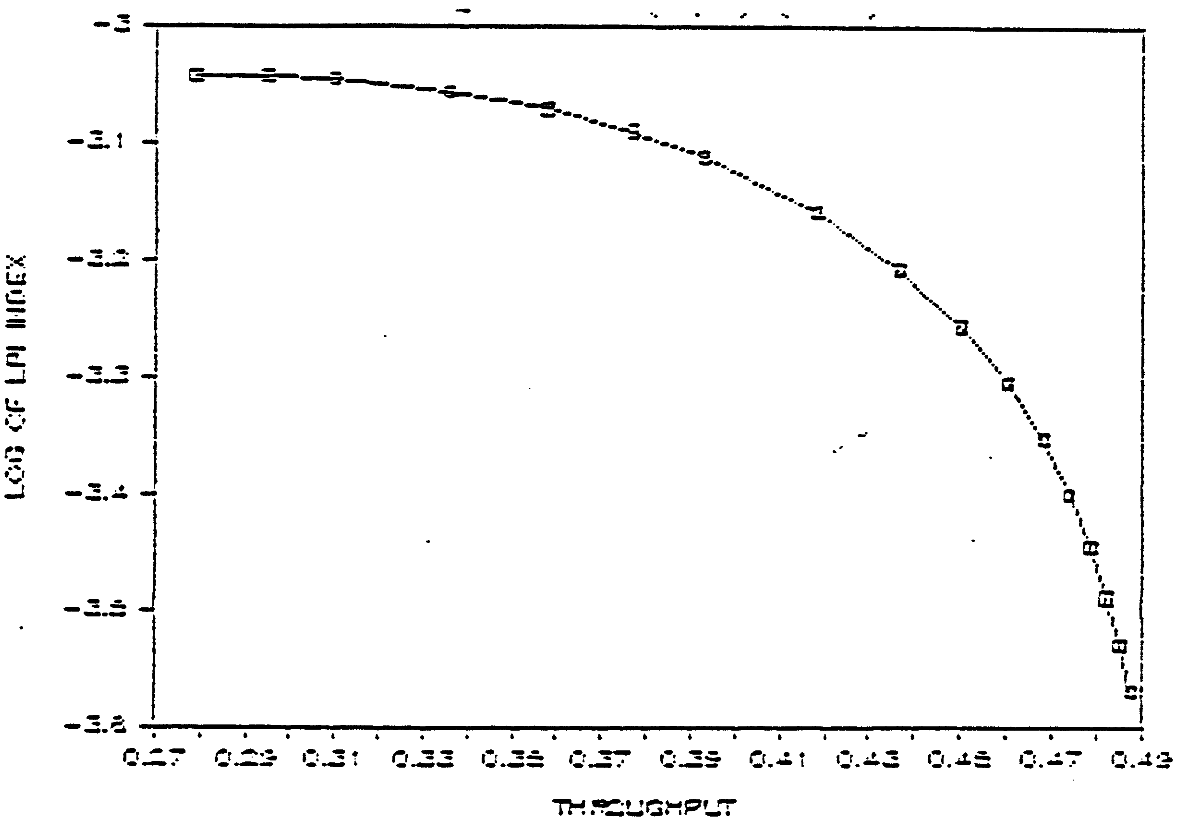

3.3 ARQ WITH CONVOLUTIONAL CODING

We now consider the case with convolutional coding. In this case, the encoder accepts blocks of $(n+h)$ bits, and encodes the whole block using convolutional codes. Strictly speaking, a truncation tail may have to be appended to each block. Nevertheless, we will ignore this for it is usually very short compared to the length of the blocks, and does not affect the results very much.

Let $P_2(d)$ be the probability of error in the pairwise comparison of two paths which differ in d bits. Let a_d be the number of paths, of distance d from the all-zero path, which merge with the all-zero path for the first time. It is widely known that the first-event error probability, ϵ, is bounded as follows. [10]

$$\epsilon \leq \sum_{d=d_f}^{\infty} a_d P_2(d) \tag{89}$$

where d_f is the free distance of the chosen convolutional code. Suppose that soft-decision decoding is used. Then, $P_2(d)$ is bounded as follows.

$$P_2(d) \leq \Big(4p(x)(1-p(x))\Big)^d \tag{90}$$

where $p(x)$ is given in (76).

From (89) and (90), we have

$$\epsilon(x) \leq \sum_{d=d_f}^{\infty} a_d \Big(4p(x)(1-p(x))\Big)^d = \hat{\epsilon}(x) \tag{91}$$

The above expression can also be written in terms of the generating sequence, $T(D)$.

$$T(D) = \sum_{d=d_f}^{\infty} a_d D^d \tag{92}$$

Thus,

$$\hat{\epsilon}(x) = T(D)|_{D=4p(x)[1-p(x)]} \tag{93}$$

Note that $\hat{\epsilon}(*)$ can be expressed as a function of x, p or D.

Given a block of $(n+h)$ bits, the probability of error is bounded as follows.

$$\varepsilon(x) \leq (n+h)\epsilon(x) \leq (n+h)\hat{\epsilon}(x) = \hat{\varepsilon}(x) \tag{94}$$

Obviously, the above bound is useful only when

$$\hat{\epsilon}(x) \leq \left(\frac{1}{n+h}\right) \tag{95}$$

From here on, we will use $\hat{\epsilon}(x)$ and $\hat{\varepsilon}(x)$ to approximate ϵ and ε respectively. For convenience, the hats will be dropped. And, no effort is made to distinguish between equality and approximate equality.

The probability that a transmitted block contains no error is

$$P_c = (1 - \varepsilon(x)) = \Big(1 - (n+h)\epsilon(x)\Big) \tag{96}$$

Hence, the throughput and the LPI index are respectively

$$\mu = R_c\left(\frac{n}{n+h}\right)\Big(1 - (n+h)\epsilon(x)\Big) \tag{97}$$

$$\lambda = \left(\frac{1}{x^2}\right)R_c\left(\frac{n}{n+h}\right)\Big(1 - (n+h)\epsilon(x)\Big) \tag{98}$$

A similar analysis as before yields the following results.

(a) $\mu_{max} = \mu(x_\mu^*, n_\mu^*) = \mu(\overline{x}, n^*(\overline{x}))$.

(b) $\lambda_{max} = \lambda(x_\lambda^*, n_\lambda^*)$ where $(x_\lambda^*, n_\lambda^*)$ solves the simultaneous equations,

$$n = n^*(x) \quad \text{and} \quad x = x^*(n)$$

(c)

$$n^*(x) = h\left\{-1 + \sqrt{\frac{1}{h\epsilon(x)}}\right\} \tag{99}$$

(d) $x^*(n)$ satisfies

$$-\left[\frac{x}{\epsilon(x)}\frac{d\epsilon}{dx}\right]\Bigg|_{x^*} = \frac{2\{1-(n+h)\epsilon(x)\}}{(n+h)\epsilon(x)}\Bigg|_{x^*} \tag{100}$$

(e) $\lambda_{\mu_{max}} = \lambda(x_\mu^*, n_\mu^*)$

(f) $\mu_{\lambda_{max}} = \mu(x_\lambda^*, n_\lambda^*)$

Lemma 3

A lower bound for n_λ^* is given by

$$n_\lambda^* = h\{w(x_\lambda^*)/2\} \geq h\{\delta(x_\lambda^*)d_f/2\} \tag{101}$$

where

$$w(x) = -\left[\frac{x}{\epsilon(x)}\left(\frac{d\epsilon}{dx}\right)\right] = -\left[\frac{x}{D}\left(\frac{dD}{dx}\right)\right]\left\{\frac{\sum d a_d D^d}{\sum a_d D^d}\right\} \tag{102}$$

and

$$\delta(x) = -\left[\frac{x}{D}\left(\frac{dD}{dx}\right)\right] = \left(\frac{\rho R_c x}{2+\rho R_c x}\right)\left(\frac{\rho R_c x}{1+\rho R_c x}\right) \tag{103}$$

Proof of Lemma 3

From (99), we have

$$\left((n+h)\epsilon(x)\right)\Big|_{n^*} = \left(\frac{h}{n+h}\right)\Big|_{n^*} \tag{104}$$

From (100) and (102), we have

$$\left((n+h)\epsilon(x)\right)\Big|_{x^*} = \left[\frac{2}{w(x)+2}\right]\Big|_{x^*} \tag{105}$$

Combining (104) and (105), we obtain

$$n_\lambda^* = h\{w(x_\lambda^*)/2\} \tag{106}$$

From (102), we have

$$w(x) \geq \delta(x)d_f \tag{107}$$

The inequality in (107) is due to the fact that

$$\sum_{d=d_f}^{\infty} d a_d D^d \geq \sum_{d=d_f}^{\infty} d_f a_d D^d \tag{108}$$

Finally, the expressions in (106) and (107) imply

$$n_\lambda^* \geq h\{\delta(x_\lambda^*)d_f/2\} \tag{109}$$

Q.E.D.

Theorem 3.1

An approximation for n_λ^* is given by

$$\hat{n}_\lambda = h\left(\frac{d_f}{2}\right) \tag{110}$$

Proof of Theorem 3.1

From (103), we know that $\delta(x)$ approaches 1 with increasing value of x. Equation (110) then follows from (109) by letting $\delta(x_\lambda^*) = 1$.

Q.E.D.

Theorem 3.2

An approximation for x_λ^* is given by

$$\hat{x}_\lambda = \epsilon^{-1}(\hat{\epsilon}_\lambda) \tag{111}$$

where $\epsilon^{-1}(*)$ stands for the inverse of the function $\epsilon(*)$, and

$$\hat{\epsilon}_\lambda = \frac{1}{h}\left(\frac{2}{d_f+2}\right)^2 \tag{112}$$

Proof of Theorem 3.2

For $x_\lambda^* \gg 2/(\rho R_c)$, $D \ll 1$, and we have

$$w(x) \approx \frac{\sum d a_d D^d}{\sum a_d D^d} \approx d_f \tag{113}$$

The proof then follows from (105), (110) and (113). Alternatively, it can also be derived from (104) and (110).

Q.E.D.

Theorem 3.3

$\mu_{\lambda_{max}}$ and λ_{max} are well approximated by $\hat{\mu}$ and $\hat{\lambda}$ respectively given below.

$$\hat{\mu} = R_c\left(\frac{d_f}{d_f+2}\right)^2 \tag{114}$$

$$\hat{\lambda} = \hat{\mu}\left\{\epsilon^{-1}\left[\frac{1}{h}\left(\frac{2}{d_f+2}\right)\right]\right\}^{-2} \tag{115}$$

Proof of Theorem 3.3

The proof follows from (97), (98), (110), (111) and (112).

Q.E.D.

As an example, consider the rate 1/2 convolutional code with $d_f = 5$ and the following generating sequence. [11]

$$T(D) = \left(\frac{D^5}{1-2D}\right) \tag{116}$$

Then,

$$\epsilon(x) = \left(\frac{D^5}{1-2D}\right)\Bigg|_{D=4p(x)[1-p(x)]} \tag{117}$$

It can be verified that

$$\sum_{d=d_f}^{\infty} da_d D^d = D\left(\frac{dT}{dD}\right) = \left(\frac{5-8D}{1-2D}\right)T(D) \tag{118}$$

It follows from (102), (92) and (118) that

$$w(x) = \delta(x)\left(\frac{5-8D}{1-2D}\right)\Bigg|_{D=4p(x)[1-p(x)]} \tag{119}$$

where $\delta(x)$ is given in (103).

Figure 14 shows the intersection between $n^*(x)$ and $x^*(n)$. The lower bound on n^*_λ is also included in the graph. The true values and corresponding approximations for x^*_λ, n^*_λ, $\mu_{\lambda_{max}}$ and λ_{max} are summarized in Table 4.

Table 4

Results for ARQ with Convolutional Coding			
x^*_λ	24.2	$\hat{x}_\lambda$	24.8
n^*_λ	77	$\hat{n}_\lambda$	80
$\mu_{\lambda_{max}}$	0.2496	$\hat{\mu}$	0.2551
λ_{max}	$4.26 * 10^{-4}$	$\hat{\lambda}$	$4.15 * 10^{-4}$

Suppose that $\overline{x} = 40$. Then, $(x^*_\mu, n^*_\mu) = (40, 332)$. It follows that

$$\mu_{max} = 0.4228 \tag{120}$$

$$\lambda_{\mu_{max}} = 2.64 * 10^{-4} \tag{121}$$

Again, the above example shows that with FEC coding, the system performance can be improved by an order of magnitude. Without FEC coding, the system performance is often not acceptable.

Figure 15 shows the Efficiency Frontier for the case with the rate 1/2 convolutional code.

Figure 14

$(x_\lambda^*, n_\lambda^*)$ FOR ARQ WITH CONVOLUTIONAL CODING

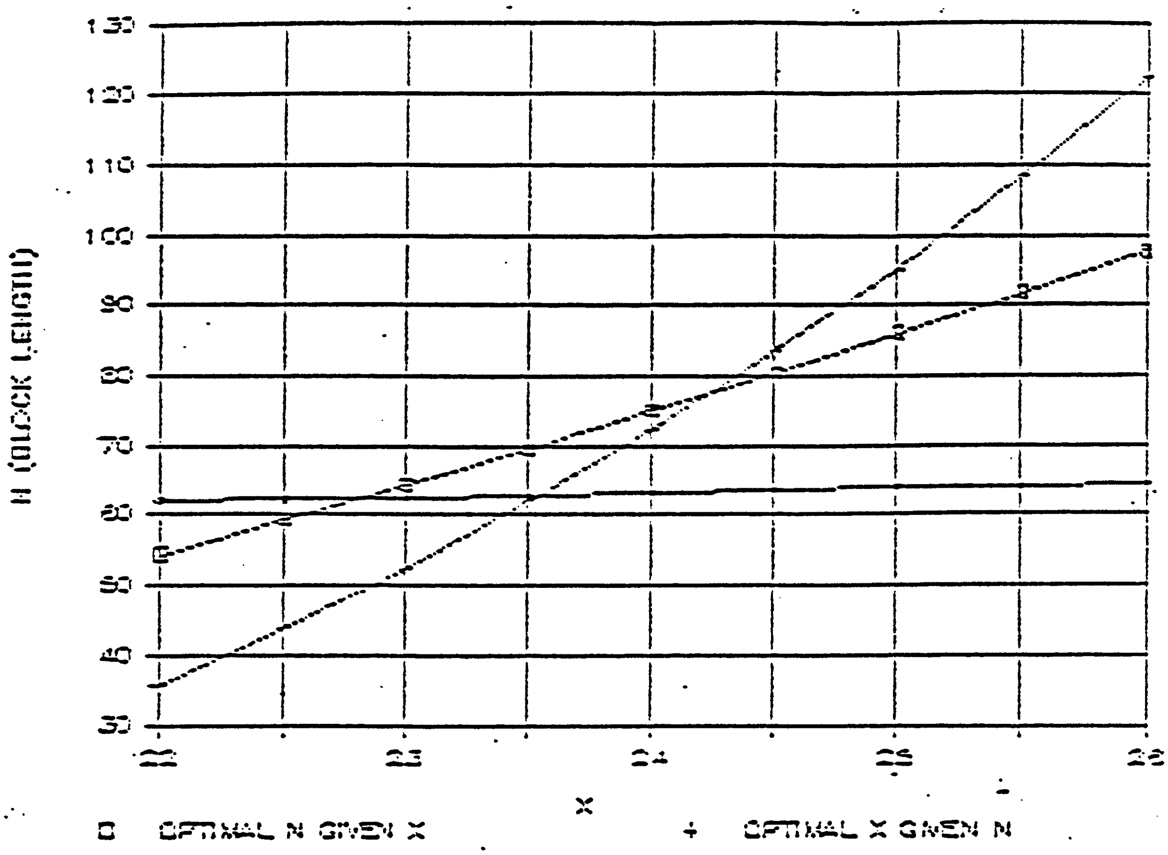

Figure 15

THE EFFICIENCY FRONTIER FOR ARQ WITH CONVOLUTIONAL CODING

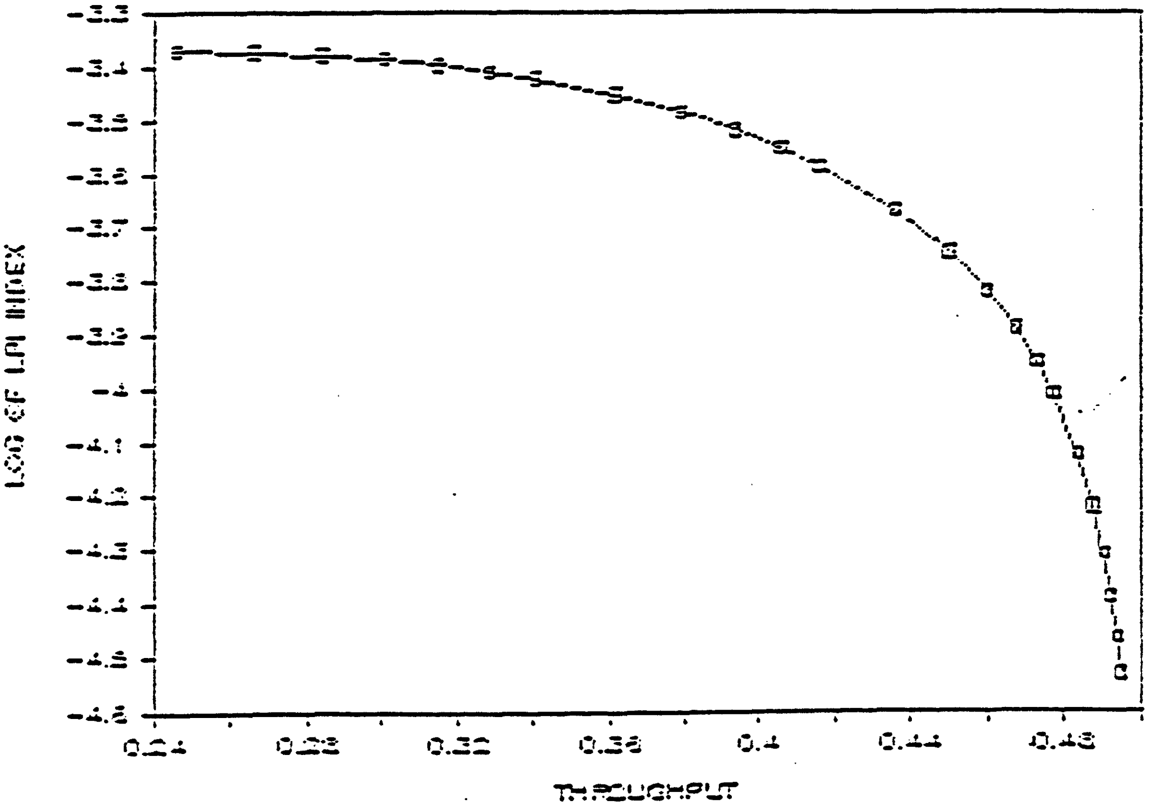

3.4 ARQ WITH TIME DIVERSITY SIGNALING

To complete the analysis, we now look at the case with time diversity signaling of order V. When non-coherent orthogonal binary FSK with square-law combining is used, the bit error probability for $x \gg V/\rho$ is given below. [10, formula 7.4.35]

$$\varphi(x) \approx \left(\frac{V}{\rho x}\right)^{V} \binom{2V-1}{V} \tag{122}$$

where V is a positive integer.

When $V = 1$, this case degenerates to the plain ARQ system. Equations (122) and (15) are, however, not exactly the same because (122) is an approximation of the actual channel bit-error-probability.

The throughput and LPI index are respectively

$$\mu = \left(\frac{1}{V}\right)\left(\frac{n}{n+h}\right)\left(1-\varphi(x)\right)^{(n+h)} \tag{123}$$

$$\lambda = \left(\frac{1}{x^2}\right)\left(\frac{1}{V}\right)\left(\frac{n}{n+h}\right)\left(1-\varphi(x)\right)^{(n+h)} \tag{124}$$

Again, a similar analysis as before leads to the following results.

(a) $\mu_{max} = \mu(x_\mu^*, n_\mu^*) = \mu(\overline{x}, n^*(\overline{x}))$

(b) $\lambda_{max} = \lambda(x_\lambda^*, n_\lambda^*)$ where $(x_\lambda^*, n_\lambda^*)$ solves the simultaneous equations,

$$n = n^*(x) \quad \text{and} \quad x = x^*(n)$$

(c)

$$n^*(x) = \frac{h}{2}\left\{-1 + \sqrt{1 - \left[\frac{4}{h\ln(1-\varphi(x))}\right]}\right\} \tag{125}$$

(d) $x^*(n)$ satisfies

$$-\left[\frac{x}{\varphi(x)}\left(\frac{d\varphi}{dx}\right)\right]\Bigg|_{x^*} = \left(\frac{2}{n+h}\right)\left[\frac{1-\varphi(x)}{\varphi(x)}\right]\Bigg|_{x^*} \tag{126}$$

(e) $\lambda_{\mu_{max}} = \lambda(x^*_\mu, n^*_\mu)$

(f) $\mu_{\lambda_{max}} = \mu(x^*_\lambda, n^*_\lambda)$

Lemma 4

An upper bound for n^*_λ is given by

$$n^*_\lambda \leq h\left\{\frac{1}{2}w(x)\left[\frac{1}{1-\varphi(x)}\right]\right\}\bigg|_{x^*_\lambda} \tag{127}$$

where

$$w(x) = -\left[\frac{x}{\varphi(x)}\frac{d\varphi}{dx}\right] = V \tag{128}$$

Proof of Lemma 4

The proof follows from the steps outlined in (38) through (43) in the proof of Lemma 1.

Q.E.D.

Theorem 4.1

An approximation for n^*_λ is given by

$$\hat{n}_\lambda = h\left(\frac{V}{2}\right) \tag{129}$$

Proof of Theorem 4.1

The bound in (127) tends to $h(V/2)$ with decreasing $\varphi(x^*_\lambda)$. For $x^*_\lambda \gg V/\rho$, $\varphi(x^*_\lambda) \ll 1$. From (125), (126) and (128), we obtain

$$n = h\left(\frac{V}{2}\right)\left\{\frac{\varphi(x)}{-(1-\varphi(x))\ln(1-\varphi(x))}\right\} \tag{130}$$

It can be verified that

$$\lim_{\varphi\to 0}\left\{\frac{\varphi}{-(1-\varphi)\ln(1-\varphi)}\right\} = 1 \tag{131}$$

Hence, (129) is a good approximation for n_λ^*.

Q.E.D.

Theorem 4.2

An approximation for x_λ^* is given by

$$\hat{x}_\lambda = \varphi^{-1}(\hat{\varphi}_\lambda) = \frac{V}{\rho}\left\{\binom{2V-1}{V}\left[\frac{V(V+2)h+4}{4}\right]\right\}^{1/V} \tag{132}$$

where $\varphi^{-1}(*)$ stands for the inverse of the function $\varphi(*)$, and

$$\hat{\varphi}_\lambda = \left\{\frac{4}{V(V+2)h+4}\right\} \tag{133}$$

Proof of Theorem 4.2

The proof follows from (126), (128) and (129).

Q.E.D.

Theorem 4.3

$\mu_{\lambda_{max}}$ and λ_{max} are well approximated by $\hat{\mu}$ and $\hat{\lambda}$ respectively given below.

$$\hat{\mu} = \left(\frac{1}{V+2}\right)\left\{\frac{V(V+2)h}{V(V+2)h+4}\right\}^{(V+2)h/2} \ll \frac{1}{V+2} \tag{134}$$

and

$$\hat{\lambda} = \hat{\mu}\left(\frac{\rho}{V}\right)^2\left\{\binom{2V-1}{V}\frac{V(V+2)h+4}{4}\right\}^{-2/V} \tag{135}$$

Proof of Theorem 4.3

The proof follows from (123), (124), (129), (132) and (133).

Q.E.D.

The intersections of $n^*(x)$ and $x^*(n)$ for $V = 2$, $V = 4$ and $V = 8$ are shown in Figures 16,17 and 18 respectively. In each of the three figures, the upper bound on n^*_λ is also included.

Figure 16

$(x_\lambda^*, n_\lambda^*)$ FOR ARQ WITH 2-DIVERSITY SIGNALING

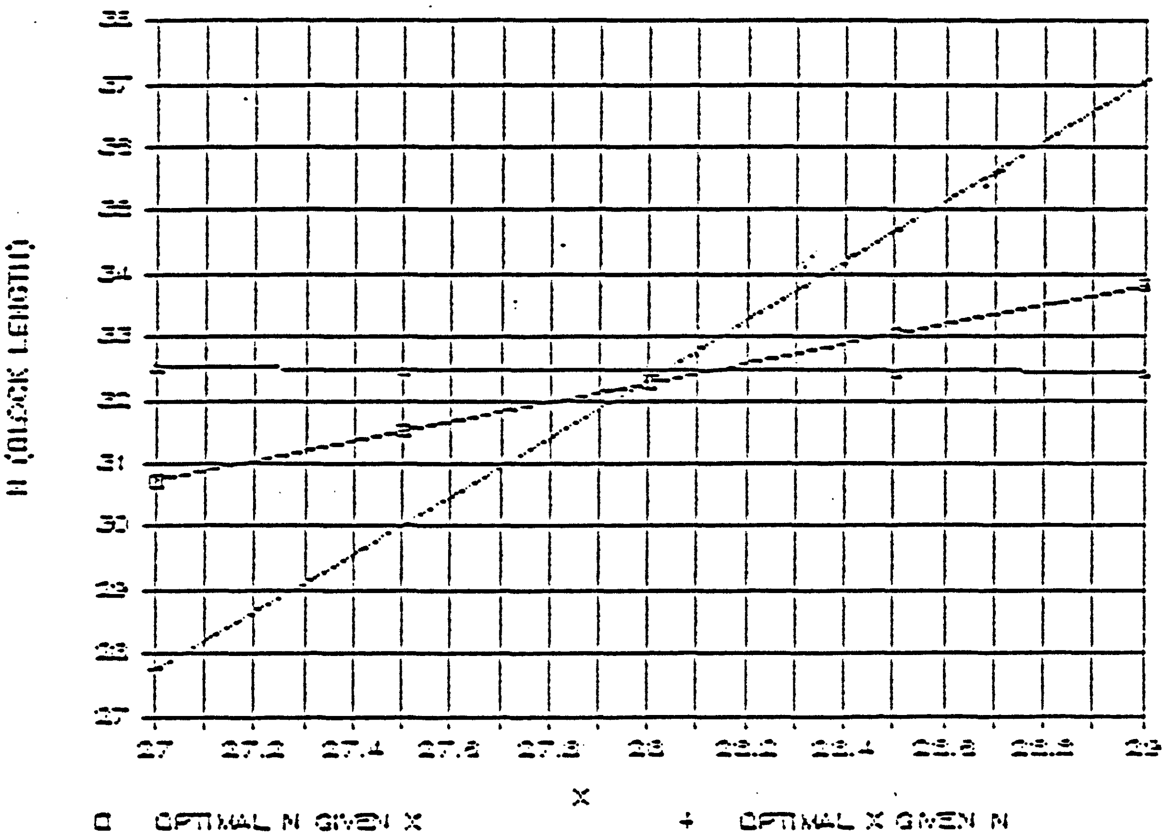

Figure 17

$(x^*_\lambda, n^*_\lambda)$ FOR ARQ WITH 4-DIVERSITY SIGNALING

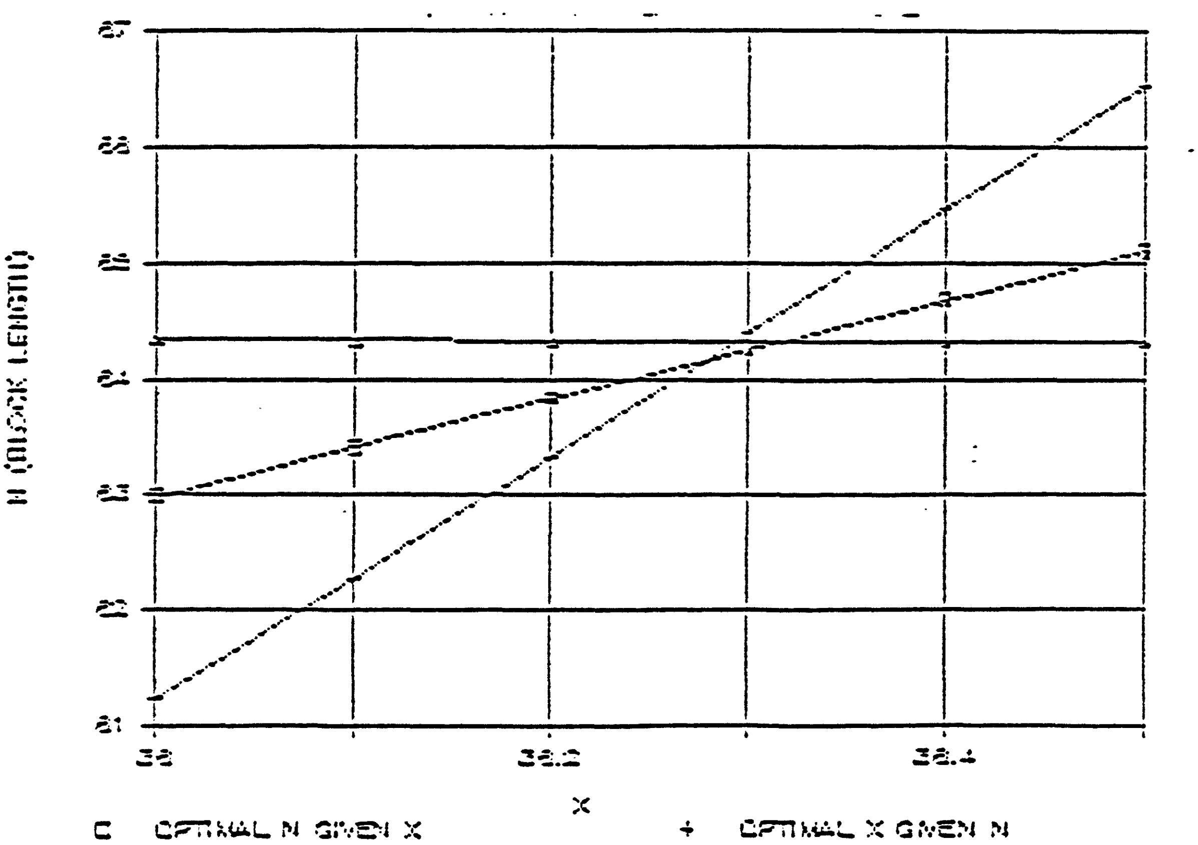

Figure 18

$(x_\lambda^*, n_\lambda^*)$ FOR ARQ WITH 8-DIVERSITY SIGNALING

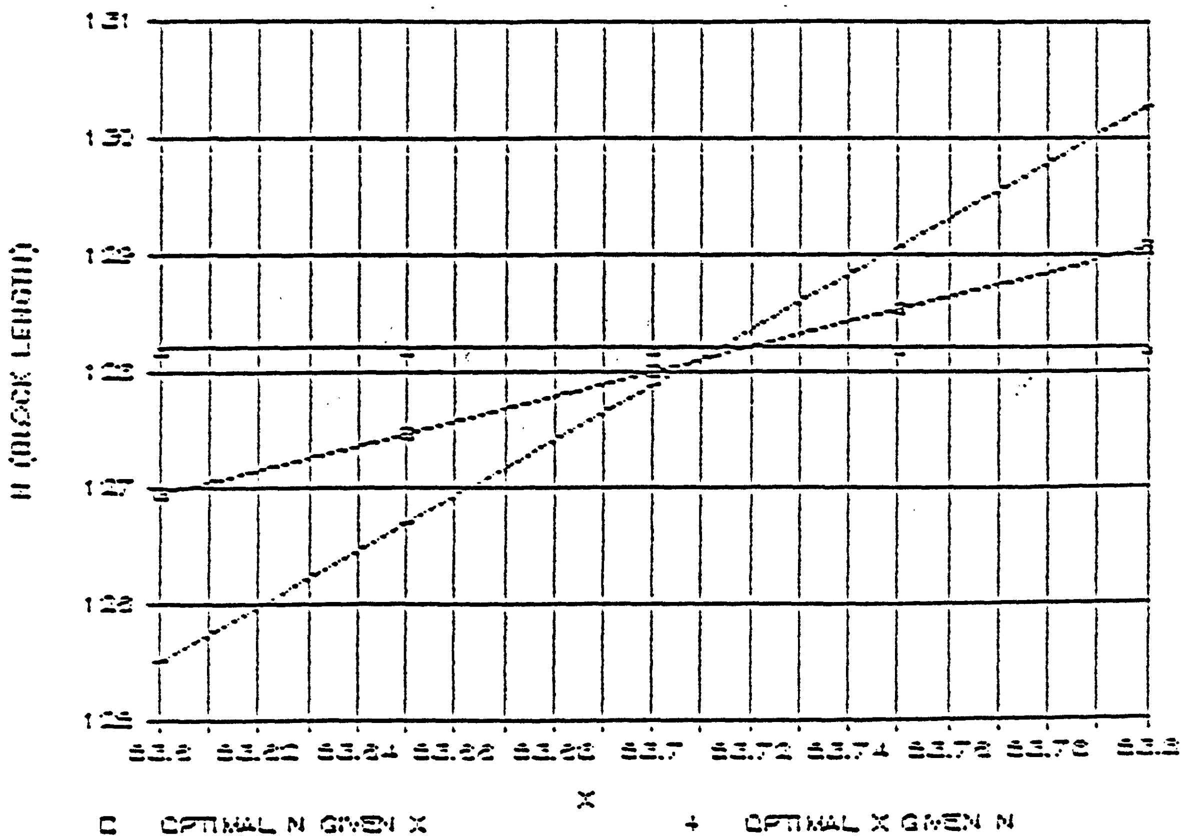

The true values and corresponding approximations for x^*_λ, n^*_λ, $\mu_{\lambda max}$ and λ_{max} are summarized in Table 5. We see that, within round-up errors, the approximations are indeed very good.

Table 5

Results for ARQ with Time Diversity Signaling			
V	2	4	8
x^*_λ	27.9	36.3	53.7
n^*_λ	32	64	128
$\mu_{\lambda_{max}}$	0.0925	0.1014	0.0778
λ_{max}	$11.88 * 10^{-5}$	$7.71 * 10^{-5}$	$2.70 * 10^{-5}$
$\hat{x}_\lambda$	27.9	36.3	53.7
$\hat{n}_\lambda$	32	64	128
$\hat{\mu}$	0.0927	0.1012	0.0779
$\hat{\lambda}$	$11.89 * 10^{-5}$	$7.70 * 10^{-5}$	$2.70 * 10^{-5}$

Suppose that $\bar{x} = 40$. Then, we obtain x^*_μ, n^*_μ, μ_{max} and $\lambda_{\mu_{max}}$ as shown in Table 6.

Table 6

x^*_μ,n^*_μ,μ_{max} **and** $\lambda_{\mu_{max}}$ **for ARQ with Time Diversity Signaling**			
V	2	4	8
x^*_μ	40	40	40
n^*_μ	51	81	31
μ_{max}	0.1645	0.1206	0.0216
$\lambda_{\mu_{max}}$	$10.28 * 10^{-5}$	$7.54 * 10^{-5}$	$1.35 * 10^{-5}$

Figure 19

THE EFFICIENCY FRONTIER FOR ARQ WITH 2-DIVERSITY SIGNALING

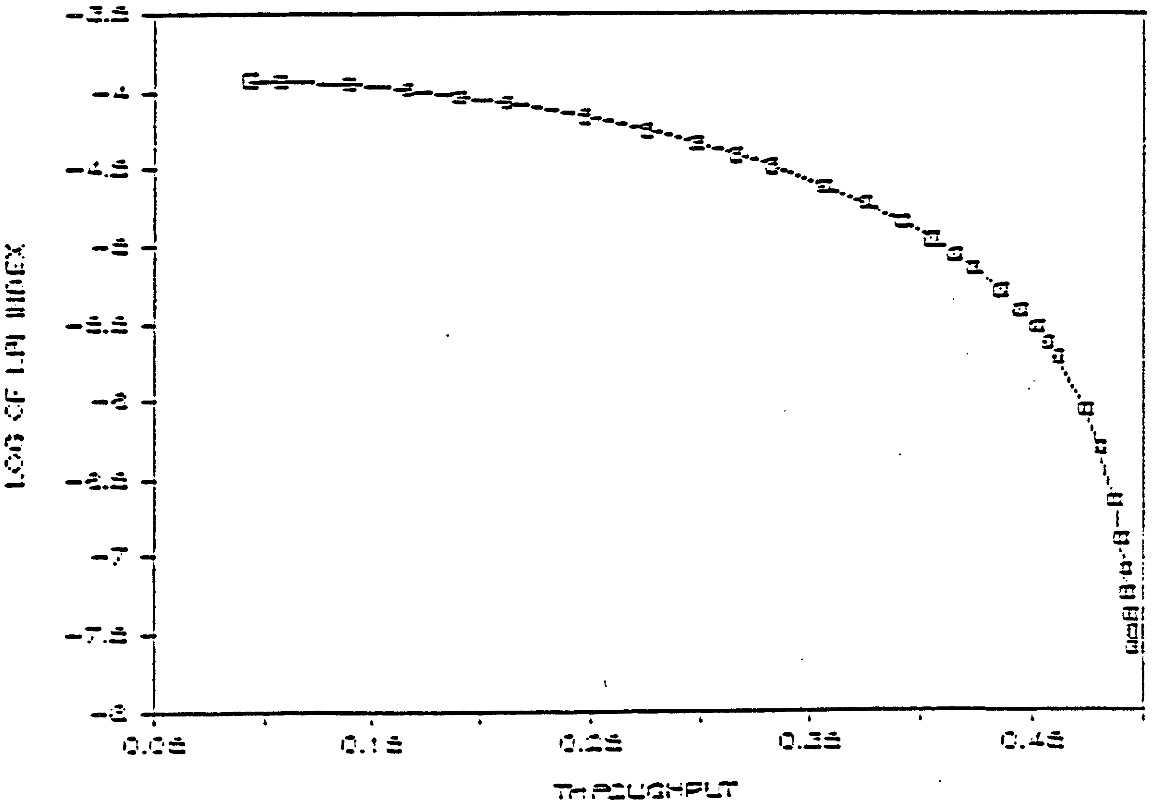

Figure 20

THE EFFICIENCY FRONTIER FOR ARQ WITH 4-DIVERSITY SIGNALING

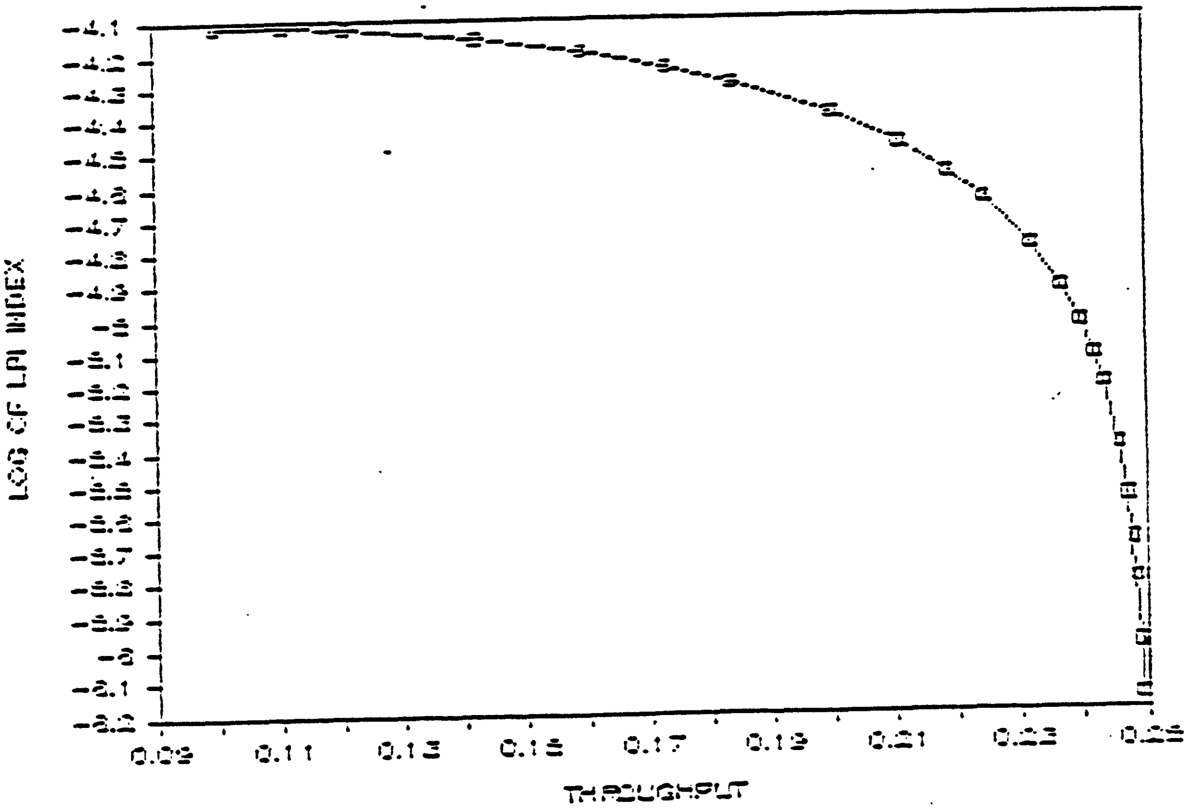

Figure 21

THE EFFICIENCY FRONTIER FOR ARQ WITH 8-DIVERSITY SIGNALING

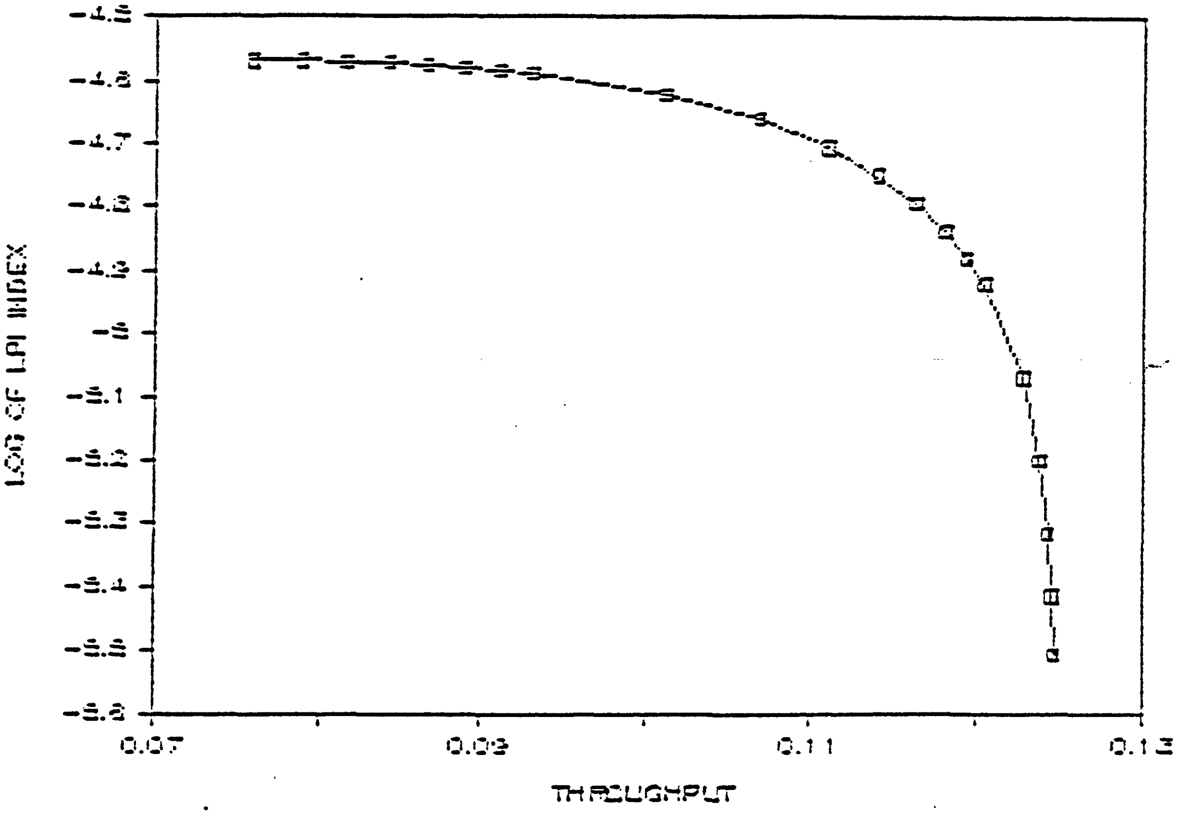

§4 SUMMARY

In this section, we summarize the analytical results presented in the previous sections. We also present some numerical results for various levels of channel attenuation and length of the header.

4.1 GENERAL FORMULATION

All the cases analyzed in the previous sections share a common general formulation. We now attempt to recapture all the important features of the models in a general framework. We will not explicitly include the operating point with maximum throughput since it can be obtained from the Efficiency Frontier.

With reference to Table 7, we have the following results.

(a) The generalized throughput is

$$\mu = R_o\left(\frac{n}{n+h}\right)\left(1-\sigma(n)\phi(x)\right)^{l(n)} \tag{136}$$

(b) The generalized LPI index is

$$\lambda = \left(\frac{1}{x^2}\right)R_o\left(\frac{n}{n+h}\right)\left(1-\sigma(n)\phi(x)\right)^{l(n)} \tag{137}$$

(c) $n^*(x)$, the optimal n given x, satisfies

$$\frac{1}{\gamma(n)}\left(\frac{h}{n+h}\right) = -\ln(1-\phi(x)) \tag{138}$$

(Note that (138) is only an approximation for the case with convolutional coding. It is a reasonably good approximation over the range of x where $\phi(x) \ll 1$.)

(d) $x^*(n)$, the optimal x given n, satisfies

$$\phi(x) = \frac{1}{\sigma(n)}\left\{\frac{2}{l(n)w(x)+2}\right\} \tag{139}$$

where

$$w(x) = -\left\{ \frac{x}{\phi(x)} \frac{d\phi}{dx} \right\} \tag{140}$$

(e) An approximation for n^*_λ is

$$\hat{n}_\lambda = h\left(\frac{\hat{w}}{2}\right) \tag{141}$$

where $\hat{w}$ is an approximation for $w(x)$.

(f) An approximation for x^*_λ is

$$\hat{x}_\lambda = \phi^{-1}\{\hat{\phi}_\lambda\} \tag{142}$$

where

$$\hat{\phi}_\lambda = \frac{1}{\sigma(\hat{n}_\lambda)} \left\{ \frac{2}{l(\hat{n}_\lambda)\hat{w} + 2} \right\} \tag{143}$$

(g) An approximation for $\mu_{\lambda_{max}}$ is

$$\hat{\mu} = R_o\left(\frac{\hat{w}}{\hat{w}+2}\right) \left\{ \frac{l(\hat{n}_\lambda)\hat{w}}{l(\hat{n}_\lambda)\hat{w} + 2} \right\}^{l(\hat{n}_\lambda)} \ll R_o\left(\frac{\hat{w}}{\hat{w}+2}\right) \tag{144}$$

(h) An approximation for λ_{max} is

$$\hat{\lambda} = \hat{\mu}\left\{ \phi^{-1}\left[\frac{1}{\sigma(\hat{n}_\lambda)} \left(\frac{2}{l(\hat{n}_\lambda)\hat{w} + 2} \right) \right] \right\}^{-2} \tag{145}$$

Table 7

Generalized System Variables				
Variables	No FEC	Block	Convolutional	Diversity
R_o	1	R_c	R_c	$1/V$
$\phi(x)$	$p(x)$	$\xi(x)$	$\epsilon(x)$	$\varphi(x)$
$\sigma(n)$	1	1	$(n+h)$	1
$l(n)$	$(n+h)$	$(n+h)/K$	1	$(n+h)$
$\gamma(n)$	n	n/K	$(n+h)$	n
$\hat{w}$	1	d_{min}	d_f	V

It is interesting to observe that $\hat{w}$, the approximation for $w(x)$, plays an important role in the approximate solutions. Moreover, it is clearly a measure of the minimum distance between transmitted words of the ARQ systems.

4.2 APPROXIMATIONS WITH LARGE VALUES OF h

For sufficiently large values of h, we further have the approximations shown in Table 8. In particular, as h tends to infinity, the approximation for $\mu_{\lambda_{max}}$ tends to $1/(3e^2)$ if no coding or diversity is used. Although the approximation is upper bounded by the code rate, R_c, significant improvement seems to be possible when FEC coding is used. For the case with time diversity, the approximation for $\mu_{\lambda_{max}}$ suggests that improvement is possible only for a small range of V.

Table 8

APPROXIMATIONS WITH LARGE VALUES OF h

	Plain ARQ	Block Coding	Convolutional Coding	Time Diversity
$l(\hat{n_\lambda})$	$3h/2$	$\frac{1}{K}\left(\frac{d_{min}}{2}+1\right)h$	1	$\left(\frac{V}{2}+1\right)h$
$\lim_{l\to\infty}\left[\frac{l\hat{w}}{l\hat{w}+2}\right]^{l}$	$\left(\frac{1}{e}\right)^{2}$	$\left(\frac{1}{e}\right)^{2/d_{min}}$	1	$\left(\frac{1}{e}\right)^{2/V}$
$\hat{\mu}$	$\frac{1}{3}\left(\frac{1}{e}\right)^{2}$	$R_c\left(\frac{d_{min}}{d_{min}+2}\right)\left(\frac{1}{e}\right)^{2/d_{min}}$ $\to R_c$ for large d_{min}	$R_c\left(\frac{d_f}{d_f+2}\right)^{2}$ $\to R_c$ for large d_f	$\left(\frac{1}{V+2}\right)\left(\frac{1}{e}\right)^{2/V}$ $\to 0$ for large V

* For $\hat{x}_\lambda \leq \bar{x}$, $\hat{\lambda} = \frac{\hat{\mu}}{\hat{x}_\lambda^2} \geq \frac{\hat{\mu}}{\bar{x}^2}$

4.3 NUMERICAL RESULTS

In this section, we substantiate our analytical results by numerical computations. Due to the lack of simple closed form expressions of the bit-error-probabilities for the ARQ systems with block or convolutional coding, we will limit our computations only to ARQ with time diversity signaling, which includes the plain ARQ system.

A simple BASIC program, to be found in the Appendix, is used to generate the Efficiency Frontier of a given ARQ system with time diversity signaling. The program can be used to model four different modulation and detection combinations. The channel bit-error-probabilities for the four combinations are given below. [10, page 470]

$$p(x) \approx \frac{1}{m\rho R_c x} \tag{146}$$

where $R_c = 1/V$ and

$$m = \begin{cases} 1 & \text{for Non-Coherent Binary FSK;} \\ 2 & \text{for Coherent Binary FSK;} \\ 2 & \text{for Binary DPSK;} \\ 4 & \text{for Coherent BPSK.} \end{cases} \tag{147}$$

The corresponding ARQ bit-error-probability is as follows. [10, section 7.4]

$$\varphi(x) = \binom{2V-1}{V}\Big(p(x)\Big)^V \tag{148}$$

While square-law combining is used with non-coherent binary FSK, maximum ratio combining is used with the other three cases.

Note that $\varphi(x)$ for $V = 1$ is only an approximation of that in (15). For large values of x, the approximation is fairly good. We will not separately use (15) for the plain ARQ system in our computations since the small difference is not worth such effort.

By letting $y = m\rho x$, it is not difficult to see from (123) and (124) that the Efficiency Frontier is shifted downwards with decreasing ρ, or upwards with increasing m. The above prediction is confirmed by the numerical results shown in Figures 22 and 23.

In Section 3.1, we predicted that the optimal LPI performance degrades with increasing length of the header. This is confirmed by the numerical results shown in Figure 24.

Figure 22

THE EFFICIENCY FRONTIERS

FOR VARIOUS CHANNEL ATTENUATION

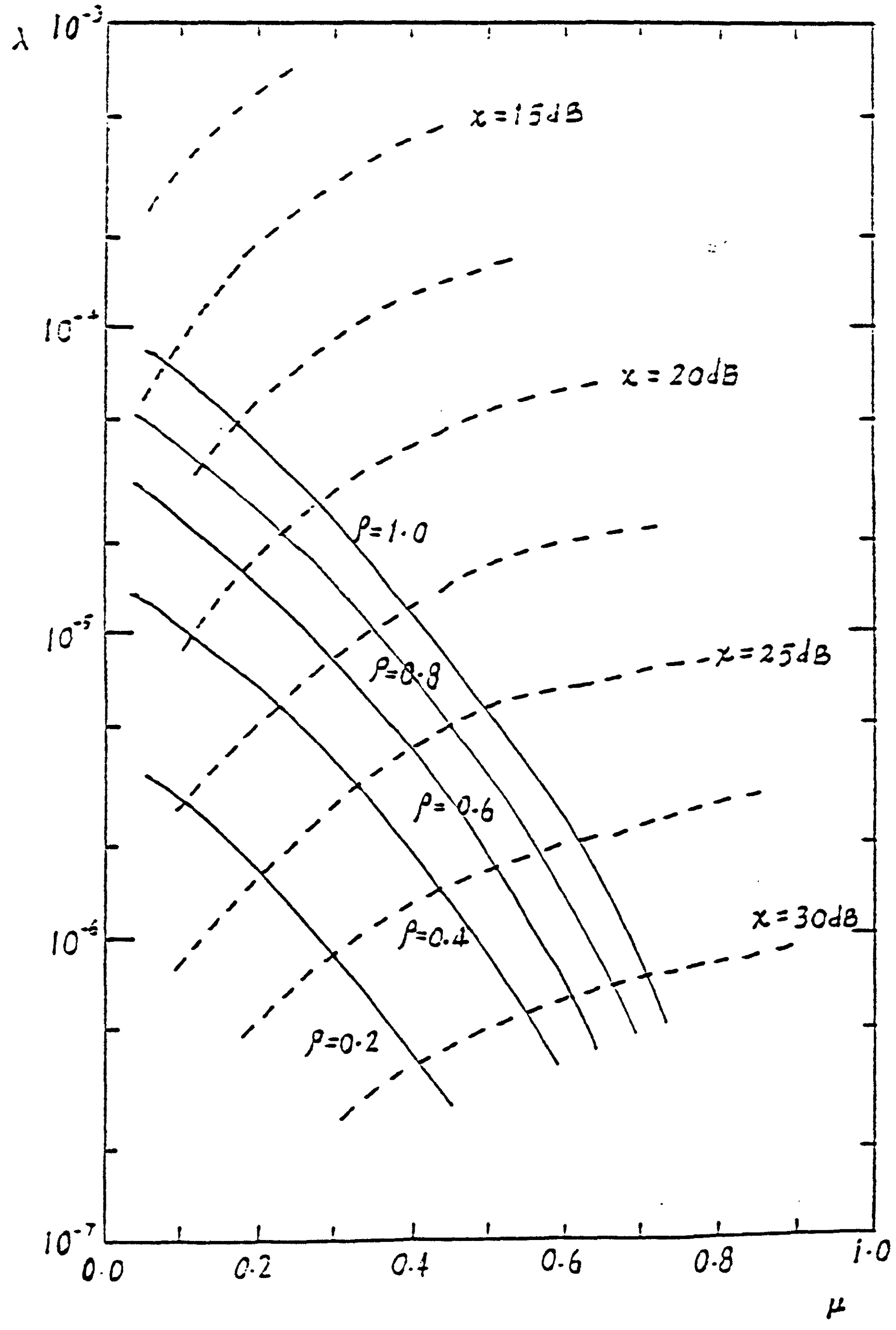

Figure 23

THE EFFICIENCY FRONTIERS

FOR VARIOUS MODEMS

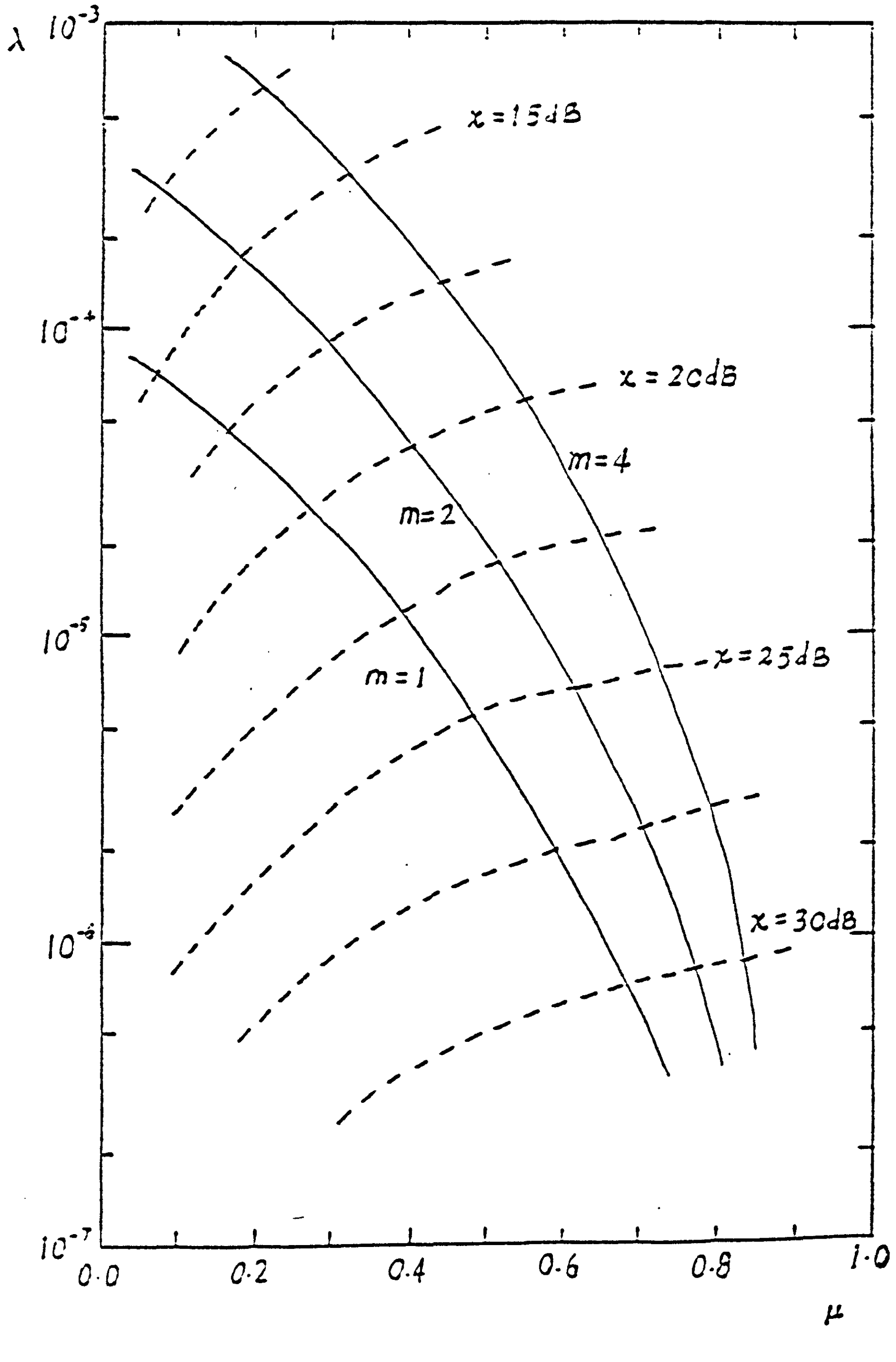

Figure 24

THE EFFICIENCY FRONTIERS

FOR VARIOUS LENGTH OF HEADER

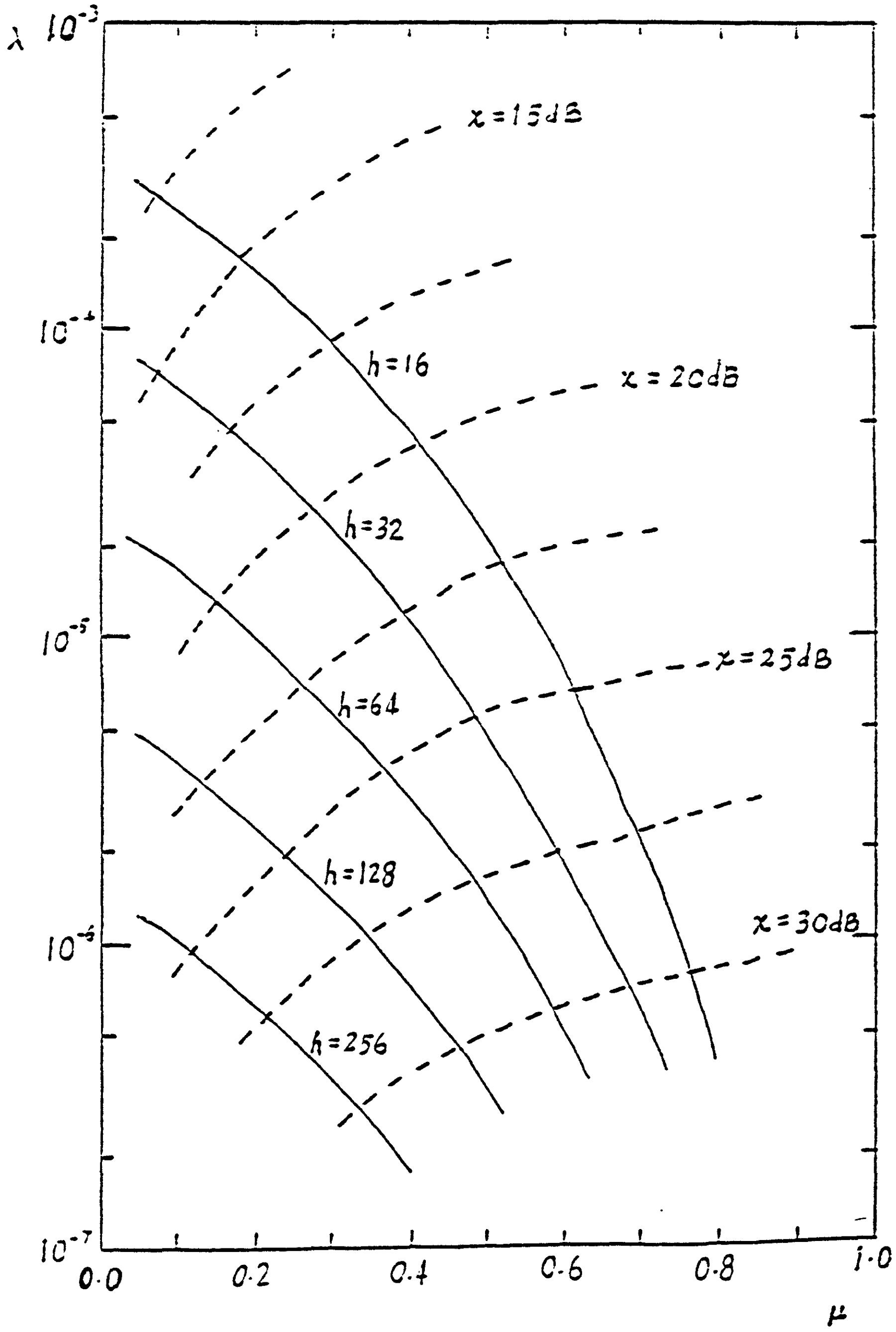

Figure 25 shows the Efficiency Frontiers for ARQ with time diversity signaling of orders 1, 2, 4 and 8. The Efficiency Frontiers for the two cases with FEC coding, considered in Sections 3.2 and 3.3, are also included for comparison. It is rather convincing that FEC coding outperforms time diversity signaling by an order of magnitude. In general, system performance, in terms of the Efficiency Frontier, degrades with increasing order of diversity. However, ARQ systems with diversity of orders 2 and 4 outperform the plain ARQ system if $\overline{x}$, the upper operating limit of x, is approximately $23dB$ and $18dB$ respectively.

Figure 25

THE EFFICIENCY FRONTIERS $(\rho = 1)$

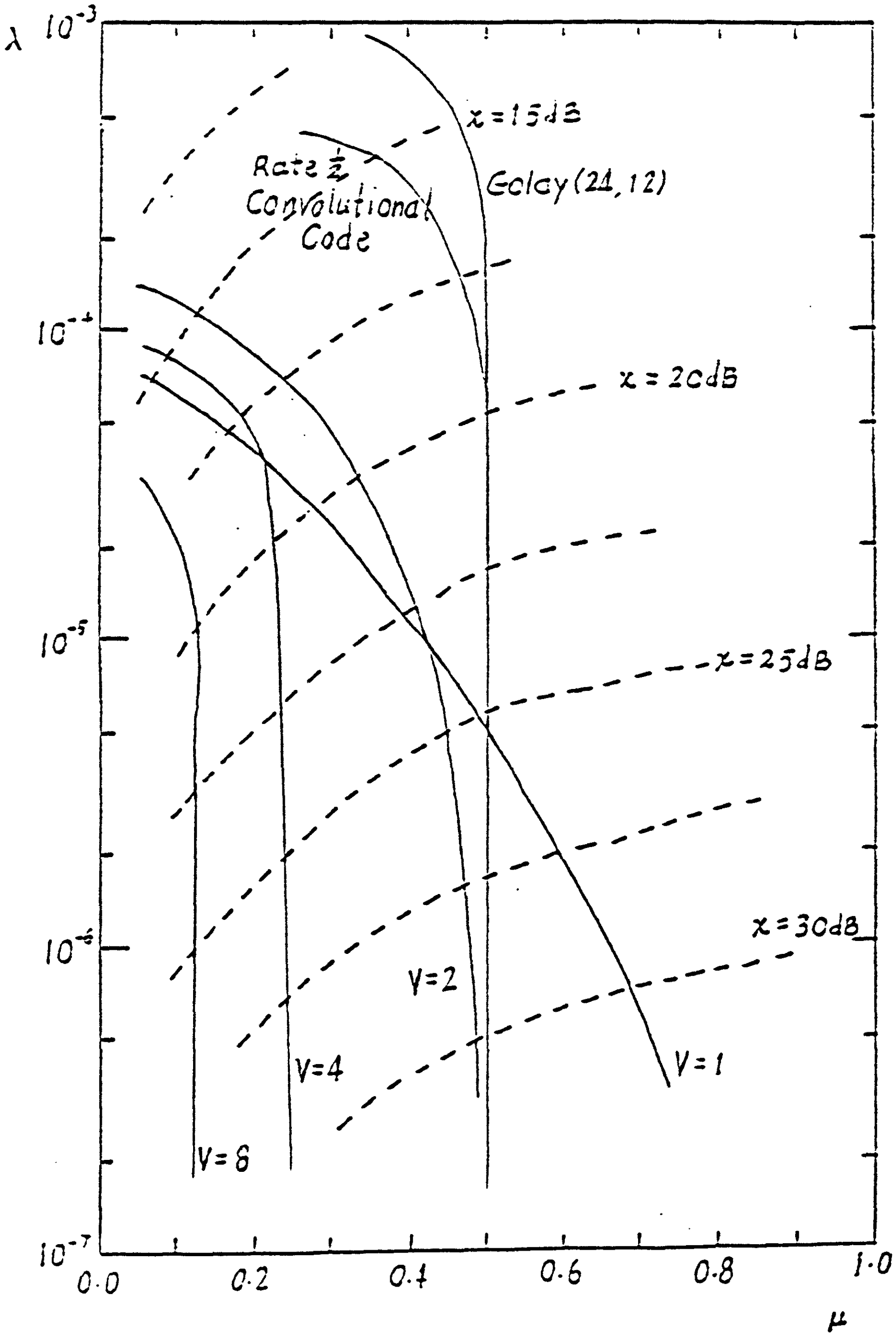

§5 CONCLUSION AND SUGGESTIONS FOR FUTURE RESEARCH

In Low-probability-of-intercept communications, there is a significant trade-off between the throughput of an ARQ system and the LPI performance. All the potential optimal operating points lie on an Efficiency Frontier, whose extreme ends correspond to the point with maximum throughput and the point with maximum LPI performance respectively.

FEC coding can be used to improve the system performance by an order of magnitude. Time diversity signaling may or may not help to improve the system performance. When the order of diversity is high, the low signaling rate dominates over the saving in retransmissions, and the system performance becomes worse than that with no diversity signaling.

In our analysis, we consider, as an example, non-coherent binary FSK signals transmitted over a Rayleigh fading channel. The generalized formulation presented in the Summary is useful for the study of cases with other modulation and detection schemes, and those operating in different channels.

A computer program has been used to generate the Efficiency Frontiers for ARQ systems with time diversity signaling operating in the Rayleigh fading channel. It is discovered that system performance generally degrades with increasing order of diversity. The computer program also incorporates different types of modems with binary signaling, namely, non-coherent FSK, coherent FSK, DPSK and coherent PSK. The numerical results show that coherent BPSK has the best performance amongst the four schemes. For operations in the fading channel, coherent BPSK is perhaps the most difficult to achieve. It appears that better throughput and LPI performance can also be achieved with sophisticated modems. System performance for various channel attenuation and length of the header has also been examined. The results are consistent with those predicted in the analysis.

In this report, several assumptions have been made to simplify the mathematics involved. More work needs to be done to relax these assumptions.

The assumption that channel bit errors are independent is not entirely realistic, especially for a fading channel. However, if fast frequency hopping and interleaving techniques are used for transmissions, this assumption may still be reasonable. Otherwise, further research in this aspect is in order.

We have considered only one type of interceptor, namely the energy detector. In practice, there are many other types of interceptors with different quality factors.

An ideal selective repeat ARQ system has been analyzed. Nonetheless, the results are to a large extent applicable to a general ARQ system, since the performance of an ideal selective repeat ARQ system provides a bound on the performance of the other ARQ systems.

§6 APPENDIX

Computer Program for generating Efficiency Frontiers

```
1000 '*********************************************************************
1002 'FILENAME: ARQDIV                                 DATE: AUGUST 1, 1985
1004 '                          WHAY CHIOU LEE
1006 '       LABORATORY FOR INFORMATION AND DECISION SYSTEMS, M.I.T.
1008 '*********************************************************************
1010 'THIS PROGRAM GENERATES THE EFFICIENCY FRONTIER OF A GIVEN ARQ SYSTEM
1020 'WITH OR WITHOUT TIME DIVERSITY SIGNALING
1040 '*********************************************************************
1050 PRINT "SPECIFY THE UPPER LIMIT OF X IN DB"
1060 INPUT LGXU
1070 PRINT "SPECIFY THE LOWER LIMIT OF X IN DB"
1080 INPUT LGXL
1090 PRINT "SPECIFY THE RESOLUTION OF THE EFFICIENCY FRONTIER IN DB OF X"
1100 INPUT RESOLUTION
1120 LET UPT = INT((LGXU-LGXL)/RESOLUTION)
1140 DIM LGX(UPT)
1160 DIM X(UPT)
1180 LET LGX(0) = LGXL
1200 LET X(0) = 10^(LGXL/10)
1220 FOR I=1 TO UPT
1240 LET LGX(I) = LGX(I-1) + RESOLUTION
1260 LET X(I) = 10^(LGX(I)/10)
1280 NEXT I
1380 '------------------------------------------------------------------------
1400 PRINT "IS DEFAULT OKAY (ANSWER YES OR NO)"
1420 INPUT SKIP$
1440 IF (SKIP$ <> "YES") THEN 2000
1480 '------------------------------------------------------------------------
1500 '>>>>>>>>>>>>>>>>>>>>>>>>>>>>>>>DEFAULT<<<<<<<<<<<<<<<<<<<<<<<<<<<<<<<<<<
1520 '>>>>>>>>>>>>>NON-COHERENT BINARY FSK WITH H=32 AND RHO=1<<<<<<<<<<<<<<<<
1530 '------------------------------------------------------------------------
1540 LET H=32
1560 LET RHO=1
1580 LET MODULATION=0
1600 LET DETECTION=0
1620 GOTO 2200
```

(continue)

```
1700 '---------------------------------------------------------------------------
2000 PRINT "SPECIFY THE LENGTH OF THE HEADER"
2020 INPUT H
2040 PRINT "SPECIFY THE VALUE OF RHO"
2060 INPUT RHO
2100 PRINT "SPECIFY THE MODULATION SCHEME (0 FOR BINARY FSK; 1 FOR BPSK)"
2120 INPUT MODULATION
2140 PRINT "SPECIFY THE DETECTION SCHEME (0 FOR NON-COHERENT; 1 FOR COHERENT)"
2160 INPUT DETECTION
2180 '---------------------------------------------------------------------------
2200 '>>>>>>>>>>>>>>>>>>>>>>>CHANNEL BIT-ERROR-PROBABILITY<<<<<<<<<<<<<<<<<<<
2215 '---------------------------------------------------------------------------
2220 '   Y = RHO*R*X
2240 '   P(X) = 1/Y                FOR NON-COHERENT BINARY FSK
2260 '   P(X) = 1/(2*Y)            FOR COHERENT BINARY FSK
2280 '   P(X) = 1/(2*Y)            FOR BINARY DPSK
2300 '   P(X) = 1/(4*Y)            FOR COHERENT BPSK
2320 '---------------------------------------------------------------------------
2480 LET M = (MODULATION+1)*(DETECTION+1)
2500 DEF FNP(Y) = 1/(M*Y)
2520 '---------------------------------------------------------------------------
6000 PRINT "ENTER ORDER OF DIVERSITY, OR 1 FOR PLAIN ARQ."
6010 INPUT V
6040 '---------------------------------------------------------------------------
6050 'GENERATING ((2V-1) CHOOSE V) FOR V=1 TO V=16
6060 'FOR THE ORDER OF DIVERSITY UP TO 16.
6068 DIM G(15)
6070 LET G(0)=1
6080 FOR I=1 TO 15
6100 LET G(I) = G(I-1)*2*(2*I+1)/(I+1)
6110 NEXT I
6120 DEF FNCHOOSE(W) = G(W-1)
6130 '---------------------------------------------------------------------------
6170 LET R = (1/V)
6180 IF V<=16 GOTO 6260
6200 PRINT "THIS PROGRAM ACCEPTS V FROM 1 TO 16 ONLY.  ";
6220 PRINT "TO CONTINUE, ENTER THE VALUE OF ((2V-1) CHOOSE V)"
6240 INPUT COEFF
6260 IF V > 16 THEN 6300
6280 LET COEFF = FNCHOOSE(V)
6290 '---------------------------------------------------------------------------
6300 '>>>>>>>>>>>>DEFINING BIT-ERRCR-PROBABILITY FOR THE ARQ SYSTEM<<<<<<<<<<<
6302 '---------------------------------------------------------------------------
6310 DEF FNPHI(S) = COEFF*(FNP(RHO*R*S)^V)
6320 IF (FNPHI(X(0)) < 1) THEN 6340
6324 'THE MODEL BREAKS DOWN WHEN THE BLOCK-ERROR-PROBABILITY, PHI(X),
6326 'IS GREATER THAN OR EQUAL TO UNITY
6328 PRINT "THE MODEL BREAKS DOWN FOR X <= "; LGX(0); " DB."
6330 PRINT "INCREASE THE LOWER LIMIT OF X AND TRY AGAIN."
6332 GOTO 9980
```

(continue)

```
6334 '----------------------------------------------------------------------
6336 '>>>>>>>>>>>>>>>>>>>>OPTIMAL BLOCK LENGTH GIVEN EB/NO (X)<<<<<<<<<<<<<<<<
6338 '----------------------------------------------------------------------
6340 DEF FNNSTAR(S) = (H/2)*(-1+SQR(1-4/(H*LOG(1-FNPHI(S)))))
6342 'THE FOLLOWING THREE STEPS PREVENT DIVIDING BY ZERO IN LINE 6340
6345 IF LOG(1-FNPHI(X(UPT))) < 0 THEN 6360
6348 PRINT "UPPER LIMIT OF X IS TOO LARGE.  TRY AGAIN"
6350 GOTO 9980
6354 '----------------------------------------------------------------------
6356 '>>>>>>>>>>>>>>>>>>>>PROBABILITY OF CORRECT TRANSMISSIONS<<<<<<<<<<<<<<<<
6358 '----------------------------------------------------------------------
6360 DEF FNPC(S) = (1-FNPHI(S))^(FNNSTAR(S)+H)
6380 GOTO 8000
6400 '----------------------------------------------------------------------
8000 '>>>>>>>>>>>>>>>>>>>>>>>>>>>>>>GENERATING OUTPUTS<<<<<<<<<<<<<<<<<<<<<<<<<
8002 '----------------------------------------------------------------------
8010 DIM N(UPT)
8020 DIM MU(UPT)
8040 DIM LAMBDA(UPT)
8060 FOR I=0 TO UPT
8080 LET N(I) = FNNSTAR(X(I))
8100 LET MU(I) = (N(I)/(N(I)+H))*FNPC(X(I))*R
8120 LET LAMBDA(I) = MU(I)/(X(I)^2)
8130 NEXT I
8132 '----------------------------------------------------------------------
8134 'APPROXIMATION OF ERROR PROBABILITY IS POOR FOR X LESS THAN ABOUT 10 DB
8138 IF LGXL >= 10 THEN 8160
8140 PRINT "WARNING! THE MODEL MAY BREAK DOWN FOR VERY LOW VALUES OF X."
8142 PRINT "CERTAIN APPROXIMATIONS USED IN THE MODEL ARE ONLY GOOD FOR X >>";
8144 PRINT USING "##.# "; 10*LOG(1/(M*RHO*R))/LOG(10);
8146 PRINT " DB."
8148 '----------------------------------------------------------------------
8150 'CHECKING TO SEE IF THE EFFICIENCY FRONTIER CAN BE GENERATED FROM ANY
8152 'PART OF THE SPECIFIED RANGE OF X.
8160 IF LAMBDA(UPT) <= LAMBDA(UPT-1) THEN 8200
8162 PRINT "WARNING! NO VALUE OF X WITHIN SPECIFIED RANGE CORRESPONDS TO ";
8170 PRINT "ANY PART OF THE EFFICIENCY FRONTIER.  INCREASE UPPER LIMIT OF X."
8180 PRINT "TRY AGAIN."
8190 GOTO 9980
8196 '----------------------------------------------------------------------
8198 'DETERMINING THE OPERATING POINT WITH MAXIMUM LPI PERFORMANCE
8200 LET PT=1
8220 WHILE (LAMBDA(PT) > LAMBDA(PT-1)) AND (PT < UPT)
8240 LET PT = PT +1
8260 WEND
8280 LPT = PT -1
```

```
8290 '-------------------------------------------------------------------------
8400 PRINT
8410 PRINT "    THE EFFICIENCY FRONTIER OF AN ARQ SYSTEM FOR LPI COMMUNICATIONS"
8420 PRINT
8430 IF M<4 THEN 8450
8440 PRINT "                              COHERENT BPSK"
8445 GOTO 8500
8450 ON (M+MODULATION) GOTO 8460,8470,8480
8460 PRINT "                            NON-COHERENT FSK"
8465 GOTO 8500
8470 PRINT "                              COHERENT FSK"
8475 GOTO 8500
8480 PRINT "                               BINARY DPSK"
8500 IF V>1 THEN 8530
8510 PRINT "                                PLAIN ARQ"
8520 GOTO 8560
8530 PRINT "              ARQ WITH TIME DIVERSITY SIGNALING OF ORDER"; V
8560 PRINT
8580 PRINT "                      LENGTH OF HEADER IS"; H;"BITS"
8600 PRINT "                            VALUE OF RHO IS";RHO
8620 PRINT
8640 PRINT "   X IN DB      X                 N               MU           LAMBDA"
8660 LET L=LPT
8680 WHILE L <= UPT
8700 PRINT USING "######.##  "; LGX(L),  X(L);
8720 PRINT USING "      #######.#         "; N(L);
8740 PRINT USING "#.####^^^^    "; MU(L), LAMBDA(L)
8760 LET L=L+1
8780 WEND
8800 PRINT
8820 PRINT "MAXIMUM LAMBDA IS ";
8830 PRINT USING "  #.####^^^^"; LAMBDA(LPT);
8840 PRINT "    AND CORRESPONDING MU IS      ";
8850 PRINT USING "  #.####^^^^"; MU(LPT)
8860 PRINT "MAXIMUM MU IS      ";
8870 PRINT USING "  #.####^^^^"; MU(UPT);
8880 PRINT "    AND CORRESPONDING LAMBDA IS ";
8890 PRINT USING "  #.####^^^^"; LAMBDA(UPT)
9980 END
9999 '***************************************************************************
Ok
```

Sample Run

```
RUN
SPECIFY THE UPPER LIMIT OF X IN DB
? 20
SPECIFY THE LOWER LIMIT OF X IN DB
? 10
SPECIFY THE RESOLUTION OF THE EFFICIENCY FRONTIER IN DB OF X
? 0.5
IS DEFAULT OKAY (ANSWER YES OR NO)
? YES
ENTER ORDER OF DIVERSITY, OR 1 FOR PLAIN ARQ.
? 1

    THE EFFICIENCY FRONTIER OF AN ARQ SYSTEM FOR LPI COMMUNICATIONS

                          NON-COHERENT FSK
                             PLAIN ARQ

                      LENGTH OF HEADER IS 32 BITS
                          VALUE OF RHO IS 1

  X IN DB       X                  N               MU           LAMBDA
   14.00      25.12              16.3         0.4743E-01     0.7518E-04
   14.50      28.18              17.8         0.5914E-01     0.7445E-04
   15.00      31.62              19.4         0.7237E-01     0.7237E-04
   15.50      35.48              21.1         0.8708E-01     0.6917E-04
   16.00      39.81              22.9         0.1032E+00     0.6512E-04
   16.50      44.67              24.9         0.1207E+00     0.6048E-04
   17.00      50.12              26.9         0.1393E+00     0.5547E-04
   17.50      56.23              29.2         0.1591E+00     0.5032E-04
   18.00      63.10              31.5         0.1799E+00     0.4518E-04
   18.50      70.79              34.1         0.2015E+00     0.4019E-04
   19.00      79.43              36.7         0.2237E+00     0.3546E-04
   19.50      89.13              39.6         0.2466E+00     0.3104E-04
   20.00     100.00              42.7         0.2698E+00     0.2698E-04

MAXIMUM LAMBDA IS    0.7518E-04    AND CORRESPONDING MU IS        0.4743E-01
MAXIMUM MU IS        0.2698E+00    AND CORRESPONDING LAMBDA IS    0.2698E-04
Ok
```

Sample Run

```
RUN
SPECIFY THE UPPER LIMIT OF X IN DB
? 20
SPECIFY THE LOWER LIMIT OF X IN DB
? 10
SPECIFY THE RESOLUTION OF THE EFFICIENCY FRONTIER IN DB OF X
? 0.5
IS DEFAULT OKAY (ANSWER YES OR NO)
? NO
SPECIFY THE LENGTH OF THE HEADER
? 32
SPECIFY THE VALUE OF RHO
? 1
SPECIFY THE MODULATION SCHEME (0 FOR BINARY FSK; 1 FOR BPSK)
? 0
SPECIFY THE DETECTION SCHEME (0 FOR NON-COHERENT; 1 FOR COHERENT)
? 0
ENTER ORDER OF DIVERSITY, OR 1 FOR PLAIN ARQ.
? 2

    THE EFFICIENCY FRONTIER OF AN ARQ SYSTEM FOR LPI COMMUNICATIONS

                            NON-COHERENT FSK
                 ARQ WITH TIME DIVERSITY SIGNALING OF ORDER 2

                        LENGTH OF HEADER IS 32 BITS
                            VALUE OF RHO IS 1

  X IN DB       X                N                 MU            LAMBDA
   14.50      28.18            32.6          0.9438E-01     0.1188E-03
   15.00      31.62            37.9          0.1166E+00     0.1166E-03
   15.50      35.48            44.0          0.1398E+00     0.1110E-03
   16.00      39.81            50.8          0.1635E+00     0.1032E-03
   16.50      44.67            58.6          0.1872E+00     0.9384E-04
   17.00      50.12            67.3          0.2106E+00     0.8285E-04
   17.50      56.23            77.1          0.2334E+00     0.7380E-04
   18.00      63.10            88.2          0.2552E+00     0.6411E-04
   18.50      70.79           100.6          0.2760E+00     0.5508E-04
   19.00      79.43           114.6          0.2957E+00     0.4686E-04
   19.50      89.13           130.4          0.3141E+00     0.3954E-04
   20.00     100.00           148.0          0.3312E+00     0.3312E-04

MAXIMUM LAMBDA IS    0.1188E-03    AND CORRESPONDING MU IS        0.9438E-01
MAXIMUM MU IS        0.3312E+00    AND CORRESPONDING LAMBDA IS    0.3312E-04
Ok
```

§7 ACKNOWLEDGEMENT

The author would like to thank Charles Stark Draper Laboratory for providing the research funding. He is also indebted to Prof. Robert Gallager and Prof. Pierre Humblet for their invaluable guidance.

§8 REFERENCES

[1] H.O. Burton & D.D. Sullivan, 'Errors and Error Control", Proc. IEEE, Vol.60, NO.11, Nov. 1972, pp1293-1301

[2] T. Klove & M. Miller, "The Detection of Errors After Error-Correction Decoding", IEEE Trans. Communications, Vol.COM-32, No.5, May 1984, pp511-517

[3] S. Lin, et.al., "Automatic-Repeat-Request Error-Control Schemes", IEEE Communications Magazine, Vol.22, No.12, Dec. 1984, pp5-17

[4] E.J. Weldon, Jr., "An Improved Selective-Repeat ARQ Strategy", IEEE Trans. Communications, Vol.COM-30, No.3, March 1982, pp480-486

[5] J.D. Edell, "Wideband, Non-Coherent, Frequency-Hopped Waveforms and Their Hybrids in Low-Probability-of-Intercept Communications", Naval Research Laboratory Report 8025, Nov. 1976

[6] A.B. Glenn, "Low Probability of Intercept", IEEE Communications Magazine, July 1983, pp26-33

[7] L.B. Sklar, "Efficiency Factors in Data Communications", IEEE Communications Magazine, Vol.22, No.6, June 1984, pp33-36

[8] J.M. Morris, "Optimal Blocklengths for ARQ Error Control Schemes", IEEE Trans. Communications, Vol.COM-27, No.2, February 1979, pp488-493

[9] W.W. Chu, "Optimal Message Blocksize for Computer Communications with Error Detection and Retransmission Strategies", IEEE Trans. Communications, Vol.COM-22, No.10, October 1974, pp1516-1525

[10] J.G. Proakis, Digital Communications, McGraw-Hill, 1983

[11] A.J. Viterbi & J.K. Omura, Principles of Digital Communication and Coding, McGraw-Hill, 1979

[12] R.G. Gallager, L.I.D.S., M.I.T., private communications

[13] P.A. Humblet, L.I.D.S., M.I.T., private communications

[14] A.S. Tanenbaum, Computer Networks, Prentice-Hall, 1981